

The Impact of High Frequency/Low Energy Seismic Waves on Unreinforced Masonry

by

Patrik K. Meyer

Submitted to the Department of Civil and Environmental Engineering
in partial fulfillment of the requirements for the degree of

Master of Science

At the

MASSACHUSETTS INSTITUTE OF TECHNOLOGY

September 2006

© 2006 Massachusetts Institute of Technology. All rights reserved.

Author *[Signature]*

Department of Civil and Environmental Engineering

August 10, 2006

Certified by *[Signature]*

John Ochsendorf

Assistant Professor of Building Technology

Thesis Co-Supervisor

Certified by *[Signature]*

John T. Germaine

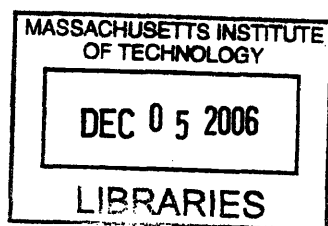
Principal Research Associate of ~~Civil and Environmental Engineering~~

Thesis Co-Supervisor

Accepted by *[Signature]*

Andrew Whittle

Chairman, Department Committee on Graduate Students



ARCHIVES

The Impact of High Frequency/Low Energy Seismic Waves on Unreinforced Masonry

by

Patrik K. Meyer

Submitted to the Department of Civil and Environmental Engineering
on August 10, 2006, in partial fulfillment of the requirements for the degree of
Master of Science in Civil Engineering

Abstract

Traditionally, the high frequency components of earthquake loading are disregarded as a source of structural damage because of their small energy content and because their frequency is too high to resonate with the natural frequencies of structures. This thesis argues that higher frequency waves travelling through stiff masonry structures can trigger two types of failure mechanisms that have not yet been taken into account. First, the high frequencies can cause small vertical inter-stone vibrations that result in irreversible relative displacements of the stones, which may ultimately lead to collapse. The energy needed to cause this deformation and failure comes largely from gravitational forces. The second failure mechanism is associated with the increase of the outward thrust that results from the partial fluidization and densification of the loose granular inner core of some unreinforced masonry walls. Preliminary results of a series of static and dynamic tests, as well as of numerical models, demonstrate the potentially destructive effects of high frequency/low energy seismic waves on unreinforced masonry structures.

Thesis Supervisor: John Ochsendorf
Title: Assistant Professor of Building Technology

Thesis Reader: Eduardo Kausel
Title: Professor of Civil and Environmental Engineering

Thesis Reader: John Germaine
Title: Principal Investigator of Civil and Environmental Engineering

Acknowledgments

I would first like to thank my advisors Assistant Professor John Ochsendorf, Dr. John Germaine, and Professor Eduardo Kausel for their support and guidance. Then, I want to thank the Hugh Hampton Young Memorial Fund Fellowship at MIT for its financial support. In addition, the NSF funds facilitated by the MIT-India program made it possible to conduct research at the Indian Institute of Technology, Bombay over the summer of 2005. I am especially thankful for the support obtained from Mr. Nissar Khan and his helpful team during the testing period on the shake table of the IITB's Laboratory of Heavy Structures. I also want to thank Tom Kachoris Jr., President of Spaulding Brick Co., Inc. and Howard Bourdelais from Modern Continental, for generously donating the bricks and materials needed to construct the walls built in the MIT laboratory. Finally, I thank Thanh-Hue Huynh, from the Technical University of Karlsruhe, for helping with the construction and testing of a number of walls.

List of Figures

FIGURE 1-1. (A) DELAMINATED STONE WALL IN AL-HOCEIMA, MOROCCO; (B) CRUMBLED CORNER OF A STONE DWELLING IN BAM, IRAN.	13
FIGURE 1-2. GRAPHICAL DESCRIPTION OF THE FAILURE MECHANISM TRIGGERED BY HIGH FREQUENCIES: (A) A TWO-WYTHE MASONRY WALL WITH A RUBBLE INFILL; (B) STONES ARE DISPLACED DUE TO VIBRATIONS; (C) INTERNAL LATERAL PRESSURE DUE TO RUBBLE IS INCREASED; AND (D) THE WALL COLLAPSES.....	14
FIGURE 1-3. A) SEISMIC HAZARD MAP OF INDIA; B) DEMOGRAPHIC MAP OF INDIA	16
FIGURE 1-4. (A) COLLAPSED ROUNDED STONE MASONRY HOUSE; (B) OUT-OF-PLANE FAILURE (SOURCE: BBC).....	17
FIGURE 1-5. WALL DELAMINATION IS A VERY COMMON FAILURE MECHANISM OF UNREINFORCED STONE MASONRY.	19
FIGURE 1-6. (A) STONE MASONRY WITH THICK JOINTS; (B) PARTIALLY DAMAGED DOME	20
FIGURE 1-7. (A) HEAVY ROOFS; (B) NO ROOF-WALL CONNECTIONS A COMMON PROBLEM.....	20
FIGURE 1-8. (A) DAMAGE TO URM STRUCTURES; (B) BUNGA HOUSE; (C) DESTROYED VILLAGE (PHOTOS: ERIC MARTI).....	22
FIGURE 2-1. COMPARISON OF SPECTRAL CONTENTS OF POKHRAN AND CHANGHAI EXPLOSIONS AT SIMILAR EPICENTRAL DISTANCES (GUPTA ET AL., 1998).....	25
FIGURE 2-2. VERTICAL GROUND VIBRATION VELOCITY AT A DISTANCE OF 4 M FROM THE COMPACTION PROBE DURING PROBE PENETRATION AND RESONANCE COMPACTION (SOURCE: MASSARSCH 2005).	26
FIGURE 2-3. PASSIVE AND ACTIVE EARTH PRESSURES; H IS THE WALL HEIGHT; Y IS THE WALL DISPLACEMENT (US ARMY CORPS OF ENGINEERS 2005).....	28
FIGURE 2-4. FREE BODY DIAGRAM OF THE FORCES ACTING ON A WALL WYTHE, INCLUDING THE VERTICAL SHEAR (V_s) AND NON-LINEAR LATERAL SOIL PRESSURE.....	29
FIGURE 2-5. QUALITATIVE COURSES OF WALL NORMAL STRESSES, AND ASSUMED TRAJECTORIES OF THE MAJOR PRINCIPAL STRESS (SOURCE: SCHULTZE 2005).....	29
FIGURE 2-6. AN EXAMPLE OF A DEM WHERE BOTH THE WALL UNITS AND THE INFILL ARE MODELED WITH DISCRETE ELEMENTS.....	32
FIGURE 3-1. THE FOUR MAIN TYPES OF SEISMIC WAVES: (A) P-WAVE; (B) S-WAVE; (C) RAYLEIGH WAVE; (D) LOVE WAVE (BRAILE).	38
FIGURE 3-2. PARAMETERS DEFINING THE PROPERTIES OF A WAVE (BRAILE).	38
FIGURE 3-3. (A) COMPARATIVE DRAWINGS OF LOOSE AND COMPACTED SOILS; (B) REDUCTION OF SHEAR MODULUS AND SHEAR WAVE VELOCITY AS A FUNCTION OF SHEAR STRAIN (RAINER MASSARSCH).....	42
FIGURE 3-4. GRAINS IN SILOS: NATURAL MASS FLOW AND ARCHING, (SCHULZE).	43
FIGURE 4-1. HORIZONTAL PRESSURES EXPERIENCED BY A RETAINING WALL TAKING INTO ACCOUNT THE ARCHING EFFECT (SOURCE: TAKE AND VALSANGKAR 2001).....	46
FIGURE 4-2. A) WALL HEIGHT NEEDED FOR SLIDING FAILURE. B) WALL HEIGHT NEEDED FOR OVERTURNING FAILURE, SHOWING THAT A MINIMUM WALL HEIGHT OF 60CM IS NEEDED TO CAUSE OVERTURNING.	47
FIGURE 4-3. A) BRICK WALL WITH TRANSPARENT INFILL BOUNDARY; B) TYPICAL STONE WALL.	51
FIGURE 4-4. GRAVEL MODELED WITH CIRCULAR CRACKS: (A) BEFORE CRUMBLING; (B) AFTER CRUMBLING, SHOWING THE ANGLE OF REPOSE.....	52
FIGURE 4-5. WALL DELAMINATION PROCESS.....	53

FIGURE 4-6.(A) STONE WALL MODEL; (B) MODEL WITH THROUGH-STONES.....	54
FIGURE 5-1. EFFECT OF FRICTION ANGLE ON FAILURE HEIGHT: INCREASING FRICTION ANGLE RESULTS IN AN INCREASE OF THE WALL FAILURE HEIGHT.	56
FIGURE 5-2. FRICTION ANGLE VERSUS STATIC AND DYNAMIC FAILURE HEIGHTS FOR BRICK WALLS: INCREASING FRICTION ANGLE RESULTS IN AN INCREASE OF THE WALL FAILURE HEIGHT.	58
FIGURE 5-3. FREQUENCIES AND ACCELERATIONS NEEDED TO INDUCE OVERTURNING FAILURE IN BRICK WALLS	58
FIGURE 5-4. A) FIRST STAGE: DENSIFICATION OF THE INFILL RESULTING IN A REDUCTION OF 10% OF INFILL HEIGHT; B) SECOND STAGE: WALL WYTHES ARE PUSHED APART DUE TO INCREASED INTERNAL PRESSURE FROM SHEAR FLUIDIZATION OF THE INFILL; C) THIRD STAGE: WALLS EITHER WHOLLY DEFORMED OR COLLAPSED.	60
FIGURE 5-5. FREQUENCIES AND ACCELERATIONS NEEDED TO CAUSE FULL FAILURE OF THE BRICK WALLS.	61
FIGURE 5-6. FAILURE FREQUENCIES AND ACCELERATIONS FOR STONE WALLS.	62
FIGURE 5-7. THE UDEC STATIC MODEL WITH COARSE GRAVEL-SIZED INFILL MATERIAL. A) INITIAL STATE OF THE MODEL JUST AFTER APPLYING THE GRAVITATIONAL FORCE TO THE MODEL; B) FAILURE ONSET AFTER TWO SECONDS; C) FAILED STATE AFTER FOUR SECONDS.....	63
FIGURE 5-8. A) PLOT OF THE IMPENDING FAILURE HEIGHT OF THE MODEL GIVEN DIFFERENT FRICTION ANGLES OF THE INFILL MATERIAL; B) ANALYTICAL MODEL USED WITH CIRCULAR INFILL.	64
FIGURE 5-9. PLOT OF THE INFILL MATERIAL'S FRICTION ANGLE NEEDED TO ALLOW FOR A GIVEN INFILL WIDTH TO BE STABLE. A 90CM HIGH MODEL WAS USED IN ALL ANALYSES.	65
FIGURE 5-10. MODELS WITH CONSTANT HEIGHT AND VARYING INFILL WIDTH.	65
FIGURE 5-11. FAILURE MODES FOR MODELS OF SAME HEIGHT AND DIFFERENT WIDTH.	66
FIGURE 5-12. HORIZONTAL ACCELERATION NEEDED TO CAUSE THE FAILURE WITH DECREASING MODEL HEIGHTS.....	67
FIGURE 5-13. VERTICAL ACCELERATION NEEDED TO CAUSE THE FAILURE WITH DECREASING MODEL HEIGHTS.....	68
FIGURE 5-14. PLOT SHOWING THE MAXIMUM ACCELERATION NEEDED TO CAUSE FAILURE OF A SPECIMEN OF A GIVEN HEIGHT.....	69
FIGURE 5-15. A) MODEL FAILING THROUGH SLIDING OF THE BRICKS; B) MODEL AFTER INITIAL ROTATION OF THE WYTHES.	69
FIGURE 5-16. (A) MODEL OF TWO-WYTHE STONE WALLS WITHOUT THROUGH-STONES; (B) MODEL WITH TWO THROUGH-STONES; (C) MODEL WITH FOUR THROUGH-STONES.	70
FIGURE 5-17. (A) FAILURE AT 0.19G; (B) FAILURE AT 0.32G; (C) FAILURE AT 0.45G.	70
FIGURE 5-18. PLOT OF THE ACCELERATION NEEDED TO CAUSE THE FAILURE OF THE MODELS WITH DIFFERENT NUMBERS OF THROUGH-STONES.....	71
FIGURE 6-1. (A) DELAMINATION OF A DRY STONE WALL WITH NO THROUGH-STONES; (B) THROUGH-STONE SOLUTION.	74
FIGURE 6-2. (A) WALL CORNER WITH THROUGH-STONES AND BIG, UNIFORM CORNER STONES; (B) THROUGH STONE MADE WITH FOUR UNITS OF SMALLER STONES.	74
FIGURE 6-3. RECOMMENDED OPENING PROPORTIONS FOR A ONE-STORY, UNREINFORCED STONE HOUSE (SOURCE: ARYA 2005).	75
FIGURE 6-4. "TEMPLES IN KYOTO WITH HANCHIKU SEISMIC ISOLATION. THE INLETS SHOW CONFINING SEAL OF CHALKY CLAY AND BASE ROCKS TO KEEP SETTLEMENTS AT ACCEPTABLE LIMITS." (SOURCE: GUDEHUS 2004)	76

FIGURE 6-5. (A) STONE LAID IN THICK MUD MORTAR; (B) DRY MUD MORTAR FALLING OUT OF THE JOINTS LEAVING VOIDS AROUND THE STONE UNITS.78

FIGURE 6-6. OUT-OF-PLANE FAILURE OF A LONG, CONTINUOUS WALL.79

FIGURE 6-7. INTRODUCTION OF CROSS-WALL TO IMPROVE THE OUT-OF-PLANE BEHAVIOR.....79

FIGURE 6-8. ROOF-WALL CONNECTION SYSTEM USING DOWELS AND WIRES (DRAWINGS BY: YANNI LOUKISSAS).80

FIGURE 6-9. ROOF-WALL CONNECTION SYSTEM USING TIMBER MEMBERS (DRAWINGS BY: YANNI LOUKISSAS).81

Note: all photos by author unless indicated.

Contents

ABSTRACT	3
ACKNOWLEDGMENTS	5
LIST OF FIGURES	6
CONTENTS	9
CHAPTER 1	12
1. INTRODUCTION	12
1.1 Background	12
1.2 Problem Statement	12
1.3 Motivation	15
1.3.1 Global Risk Assessment	15
1.4 Masonry Behavior in Recent Earthquakes	16
1.4.1 Kashmir – Pakistan	17
1.4.2 Bam – Iran	19
1.4.3 Bhuj – India	21
1.5 Discussion	22
1.6 Thesis Outline	23
CHAPTER 2	24
2. LITERATURE REVIEW	24
2.1 High Frequency Seismic Vibrations and Masonry Structures	24
2.2 Shear Fluidization of Granular Soils	26
2.3 Granular Soil-Structure Interaction	27
2.3.1 Retaining Walls	27
2.3.2 Silos	29
2.4 Conventional Methods to Analyze URM	30
2.4.1 Finite Elements Method: FEM	30
2.4.2 Discrete Elements Method: DEM	31
2.4.3 Distinct Panels	32
2.4.4 Probabilistic Risk Assessment	33

2.5	Discussion	34
CHAPTER 3		35
3.	BACKGROUND INFORMATION AND THEORY	35
3.1	Unreinforced Stone Masonry (URSM): Advantages and Disadvantages	35
3.1.1	Advantages	35
3.1.2	Disadvantages	36
3.2	Unreinforced Brick Masonry (URBM): Advantages and Disadvantages	36
3.2.1	Advantages	36
3.2.2	Disadvantages	37
3.3	Seismic Waves	37
3.4	Frequencies	39
3.5	Shear Fluidization and Ratcheting	40
3.6	Compaction of Dry Granular Soils	41
3.7	Arching Phenomenon	42
3.8	Discussion	43
CHAPTER 4		45
4.	METHODOLOGY	45
4.1	Preliminary Evaluation	45
4.2	Static Tests: Brick Walls	48
4.3	Dynamic Test: Brick and Stone Walls	49
4.3.1	Vertical Vibrations	49
4.3.2	Horizontal Vibrations	50
4.4	Analytical Models: Brick Walls	51
4.5	Analytical Models: Stone Wall Delamination	52
4.6	Discussion	54
CHAPTER 5		56
5.	RESULTS	56
5.1	Static Tests: Brick Walls	56

5.1.1	Influence of Granular Infill Friction Angle	56
5.2	Dynamic Tests	57
5.2.1	Vertical Vibrations: Brick Walls	57
5.2.2	Horizontal Vibrations: Brick Walls	59
5.2.3	Horizontal Vibrations: Stone Walls	61
5.3	Analytical Model	62
5.3.1	Static Conditions	62
5.3.2	Dynamic Conditions	66
5.4	Discussion	71
CHAPTER 6		73
6.	LOW-COST REMEDIAL ACTIONS	73
6.1	New Construction	73
6.1.1	Through-Stones and Stone Shape	73
6.1.2	Distribution and Proportions of Openings	75
6.1.3	“Hanchiku” Seismic Base Isolation	75
6.2	Retrofit	77
6.2.1	Through-Stones and Cementitious Mortar	77
6.2.2	Room Partitions	78
6.2.3	Roof-Wall Connection I	79
6.2.4	Roof-Wall Connection II	80
6.3	Discussion	81
CHAPTER 7		83
7.	CONCLUSIONS AND FUTURE WORK	83
BIBLIOGRAPHY		85
APPENDIX 1: UDEC SCRIPTS		88
APPENDIX 2: PAMPHLET DISTRIBUTED IN KASHMIR 06		90

Chapter 1

1. Introduction

1.1 Background

In developing countries, more unreinforced masonry structures exist than any other type of structure (UN-Habitat 2005), and such structures are the least seismically safe (Government Code 2004). Recent earthquakes, such as those in Pakistan (2005), Bam (2003) and Gujarat (2002), have raised awareness of the need for scientific methods to assess the structural integrity of unreinforced construction under seismic loading, and of methods to increase their performance. Years of earthquake research and laboratory testing have demonstrated that houses and buildings built with brittle materials are intrinsically unsafe under seismic loading and require remedial reinforcement to guarantee an acceptable degree of ductility. Despite this research, however, the actual failure mechanisms of brittle masonry construction remain obscure and poorly understood. The methods used in developing countries for low cost construction are highly variable and based on empirical rules rather than on an understanding of structural behavior and performance. Because of the inherent complexity and variability in masonry materials and construction methods, such structures are difficult to model effectively with numerical methods. Current analytical methods are based on a number of major simplifications, such as the pure brittle behavior and isotropy of masonry. These simplifications lead to models that often are not representative of the actual structures, and it is difficult, if not impossible, to determine the many structural and constitutive parameters needed for such numerical models. This is especially true in seismic situations, which involve loading and unloading, fracture propagation, contact and slip, and other considerations.

1.2 Problem Statement

From our observations in the field, we have learned that the failure mechanisms often involve the aggregation of irreversible “stick-and-slip” processes between bricks or stones (Kolb et al. 1999). The stick-and-slip process results in a gradual release of gravitational energy and dislocation of structural elements from their stable positions in walls (Figure 1-1). Frequencies higher than 10

Hz could be the source of these processes and may cause two failure mechanisms that have not yet been accounted for.

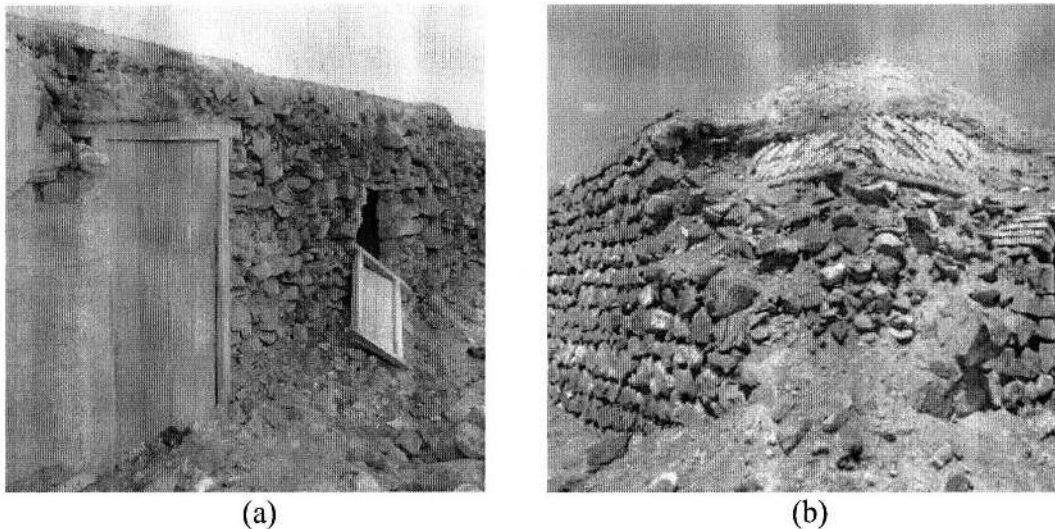


Figure 1-1. (a) Delaminated stone wall in Al-Hoceima, Morocco; (b) Crumbled corner of a stone dwelling in Bam, Iran.

The first failure mechanism affects stone masonry structures and is triggered by high frequency vibrations that excite inter-stone vibrations. Relative displacement of the stones may accumulate from repeated stick-slip processes elicited by these vibrations, inasmuch as the stones are frequently oblong or pyramidal, with their bases oriented toward the exposed part of the wall (Fig. 2a). Their irregular shape facilitates the irreversible downward sliding of the stones, leading to a relative displacement of the masonry units (Figure 1-2b-c). As a consequence of this relative movement of the stones, the wall becomes deformed and unstable, leading to catastrophic collapse under its own weight.

The energy needed to cause this deformation and failure mechanism does not come predominantly from the earthquake waves, as is commonly assumed, but from the release of the potential energy stored in the structure. That is, the energy needed to cause the collapse of the structure comes from the structure itself. Hence, small energy, high frequency seismic waves can trigger the collapse mechanism of poorly built walls. Furthermore, the damaging effects of higher frequencies are amplified by the fact that for frequencies higher than 10Hz, the vertical

accelerations are larger than the horizontal ones (Singh 2005), a situation that further reduces the inherent cohesion of the masonry.

A second unaccounted for failure mechanism is associated with the increase in outward thrust from the densification and fluidization—loss of shear strength due to particle vibrations—of the wall’s inner core granular material. In masonry walls, the inner core is often made up of loose sand and gravel that tend to densify and fluidify when experiencing high-frequency vibrations (Svinkin 2005), resulting in a significant increase of the lateral thrust. This additional thrust will push the unstable masonry units outward causing the deformation and possible collapse of the masonry skins. This failure mechanism will compound the effect of the previously described inter-stone displacement elicited by the high frequency motion components, as depicted in Figure 1-2.

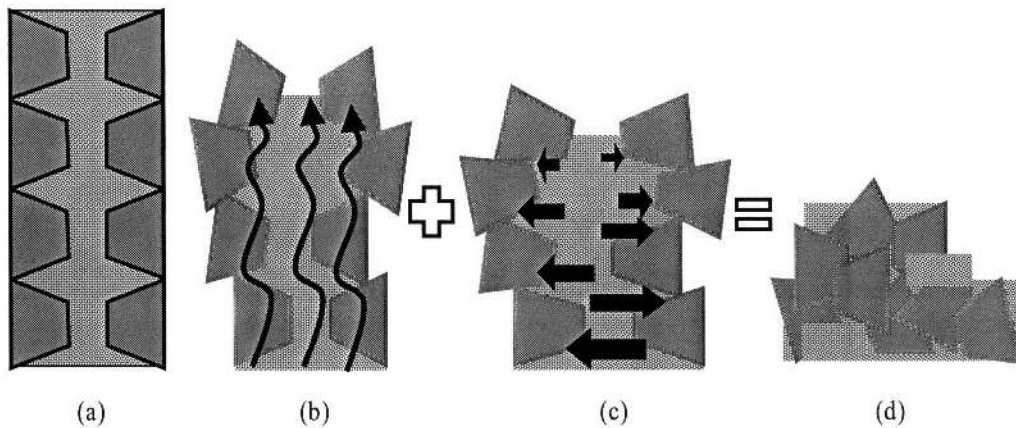


Figure 1-2. Graphical description of the failure mechanism triggered by high frequencies: (a) A two-wythe masonry wall with a rubble infill; (b) stones are displaced due to vibrations; (c) internal lateral pressure due to rubble is increased; and (d) the wall collapses.

To study the failure mechanisms described above, a series of laboratory scale brick walls were built and tested to identify the heights at which the walls were statically stable with different sized infill. Then, a second series of similar brick walls, as well as a number of stone walls were tested to observe their dynamic behavior. Finally, UDEC, a discrete element modeling software, was used to analyze the brick walls and compare the results with those obtained experimentally. The results obtained from this research validate the significance of the damaging effects of higher frequencies on the overall structural stability of unreinforced masonry.

1.3 Motivation

1.3.1 Global Risk Assessment

With over 2.8 billion people living on less than \$2 a day and almost half of them on less than \$1 a day, there is a dire need in developing countries for no-cost housing. It is estimated that “1.1 billion people are living in inadequate housing conditions in urban areas alone.” (UNCHS 1999) In addition, some 35 million housing units each year would be needed to fill the current housing deficit and meet the growth of households in developing countries. Buying expensive construction materials is not an option for the majority of the people living on and under the poverty line. Therefore, they have to make recourse of their ingenuity and the materials they can gather in their environment. Two construction materials that are readily available to them are soil and stones. These materials can be safely used as construction materials if employed appropriately in non-seismic regions. However, in seismic-prone regions, the performance of unreinforced dry stone masonry and brick masonry is poor. Hence, it is imperative to follow much stricter construction rules than in non-seismic regions to build safe structures.

To illustrate the magnitude and urgency of this situation, the case of the Indian housing condition will be analyzed next in more details. The Indian Subcontinent with a population of over 1.1 billion is one of the most disaster-prone regions in the world (BMTPC 2000):

- 54% of land is vulnerable to earthquakes
- 8% of the land is vulnerable to cyclones
- 5% of the land is vulnerable to floods

These hazards cause the damage or destruction of over one million houses per year, with consequent human, social, and economic impact. Figure 1-3a) shows the seismic hazard map for India and Figure 1-3b) shows the population map of India. From these two maps it can be observed that over 30% of the country’s population (330 million) lives in seismically active regions. 85% of India’s building stock –165 million housing units- is composed of earthen, brick, and stone buildings (Arya 2005). Taking into account that more than 80% of the Indian building stock is not seismically safe, over 280 million people are living in 50 million homes that are at risk of being severely damaged or destroyed during a moderate to strong earthquake. These 50 million homes are either unreinforced brick or stone masonry. In the cases where

reinforcement is part of the structure, which is often poorly designed and insufficient to carry dynamic loads, masonry is still used as infill material within the reinforced frame.

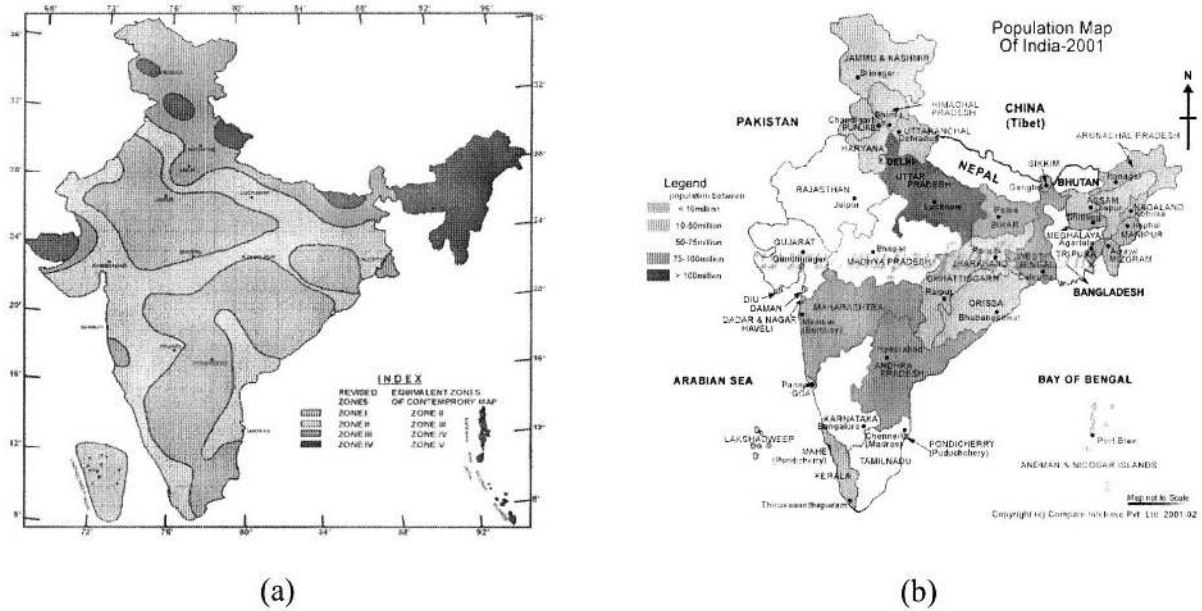


Figure 1-3. a) Seismic Hazard Map of India; b) Demographic Map of India

Many of the developing countries in Central-Asia, China, and Central and South-America are in a similar hazardous situation as India, resulting globally in more than one billion people living in mostly unreinforced or poorly reinforced masonry houses in seismic regions. An improved understanding of unreinforced masonry (URM) structures under seismic loads is crucial to be able to build safer house and design effective retrofit schemes.

1.4 Masonry Behavior in Recent Earthquakes

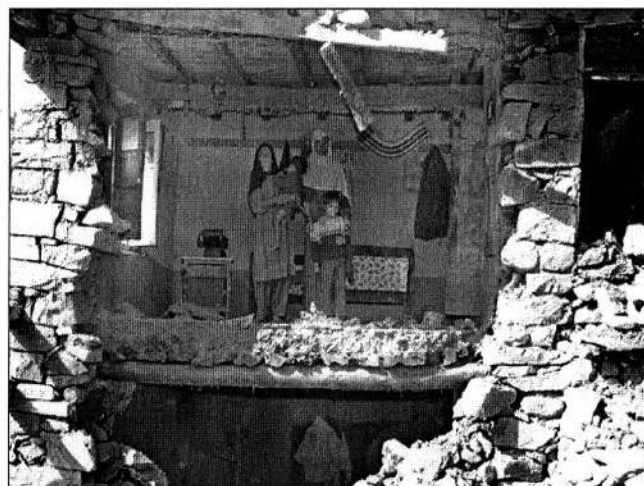
In this section the performance of URM in three recent earthquakes is assessed. These three earthquakes occurred within a time frame of six years in different parts of the world and caused between 35000 and 90000 deaths each. The number of casualties would climb at least an order of magnitude if a strong earthquake were to hit a large metropolis like Teheran, Istanbul, or New Delhi.

1.4.1 Kashmir – Pakistan

The most recent major earthquake occurred in the region of Kashmir in Pakistan on October 8th 2005. This magnitude 7.6 earthquake killed over 80,000 people, injured 200,000, and left over four million homeless. A large share of the casualties and injuries in this rural region of Northern Pakistan were the result of the collapse of unreinforced single-storey stone and brick masonry buildings. Stone masonry houses are widespread in villages in the mountainous region of Kashmir where stone is readily available. Stone masonry walls were poorly built with undressed stones placed irregularly. In addition, the stones were often rounded (Figure 1-4a), further weakening the overall stability of the house. The stones were often set in plain mud or at best in 1:10 sand/cement weak mortars (EERI 12/2005). This weak mortar was crushed during the seismic loading, leaving gaps between the stones that accelerated the collapse of the houses. Out-of-plane failure was another common failure mechanism observed during this earthquake (Figure 1-4b).



(a)



(b)

Figure 1-4. (a) Collapsed rounded stone masonry house; (b) out-of-plane failure (Source: BBC)

As in most earthquakes, stone masonry structures performed very poorly during the Kashmir earthquake. Three main structural reasons are the source of this poor performance. First, stone walls are often built using two individual wythes that are not interconnected (Figure 6-1) which allows them to act as two independent units, resulting in the delamination of the wall and its

crumbling. A second problem is that the area of the openings (windows and doors) is too large, inadequately spaced, and unevenly distributed around the structure. This facilitates the initiation and propagation of cracks, as well as the induction of torsional forces into the structure due to stiffness eccentricities. The third major problem of this type of structure is that the individual walls of the houses act independently of each other because there are no structural bands to tie them together. This weakens the overall structure and results in the out-of-plane partial or total collapse of the walls. Properly tying down the rigid roof to the walls would effectively bond together the exterior walls, resulting in a box action of the overall structure and therefore reducing the risk of out-of-plane failure of the individual walls (CUL 2005).

Wall delamination is a commonly observed failure mechanism of unreinforced stone masonry under seismic loading. In the recent earthquake in Northern Pakistan (10/2005) most of the rural housing, 88% of the total housing stock in the region, and a significant number of urban structures were built with stone load-bearing walls. As can be observed in Figure 1-5a, stone walls are built with two *disconnected* wythes, which in case of a seismic event, act as individual units. Wall delamination is facilitated by the use of rounded stones (Figure 1-5b). In mountainous regions where stones are easily available, unreinforced masonry is also used in the construction of upper-scale housing and public facilities (Figure 1-5c), which in case of the Pakistan earthquake resulted in the collapse of schools and hospitals. Until recently it was believed that wall delamination would mainly occur in houses with heavy roofs; however, most of the rural housing units damaged in Kashmir/Pakistan had a light roofing system and the walls still failed (Figure 1-5d and e).



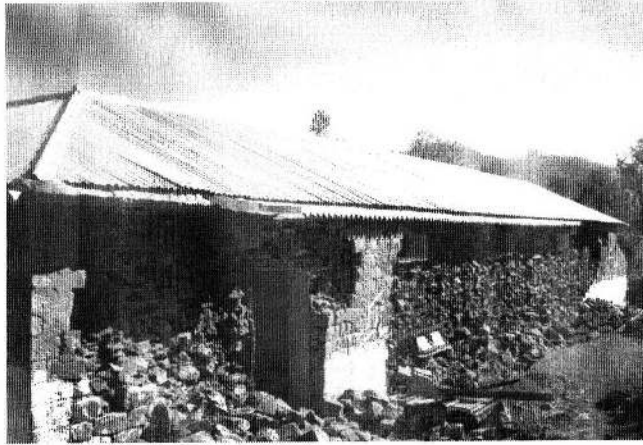
(a)



(b)



(c)



(d)



(e)

Figure 1-5. Wall delamination is a very common failure mechanism of unreinforced stone masonry.

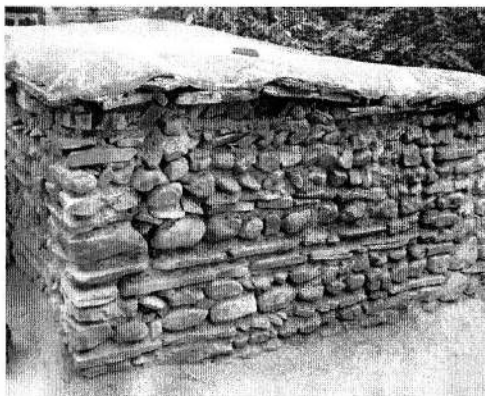
1.4.2 Bam – Iran

The December 2003 Bam 6.6 (Ms) earthquake was particularly fatal. Approximately 30% of the 90,000 strong population of Bam was killed and almost the totality was rendered homeless. Before the earthquake, Bam was a prosperous small city. Yet, it took the earthquake less than one minute to convert this wealthy and beautiful oasis into a pile of rubble. Over 45,000 people were killed and 50,000 mostly unreinforced dwellings were destroyed in the region of Bam. The most common construction materials used is adobe and solid earthen-fired bricks. The dwellings built with these materials consisted of massive adobe bearing walls with vaulted or domed roofs (Figure 1-6b). In the cases where stones were used, they were laid on thick mud-mortar joints, making the structure very vulnerable to crumbling (Figure 1-6b). The most common failure mechanisms were the out-of-plane failure and crumbling of the walls, followed by the collapse of the heavy roofs (Figure 1-7a). It is interesting to note that many roofs were built using steel beams. Unfortunately the beams were simply put on top of the walls with no further connection between them (Figure 1-7b). This allowed the out-of-plane failure of the walls followed by the collapse of the roof.

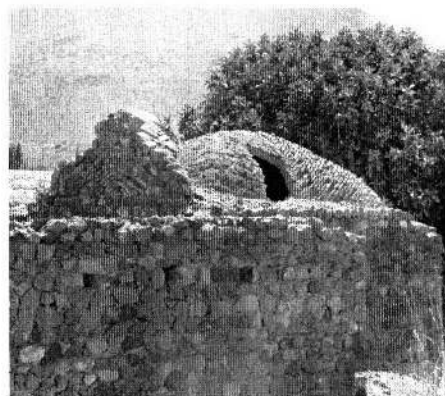
The Bam earthquake not only destroyed the city of Bam but also the 2000-year-old citadel, Arg-e-Bam. Both the city and its citadel are sitting on top of the Bam thrust fault. It is believed that many ancient and newer URM structures were destroyed due to the horizontal accelerations combined with the vertical ones, which in this case peaked at around 1g. This high

vertical acceleration component resulted in the structures experiencing internal vertical absolute forces that oscillated from none to twice their self-weight. The frictional forces between the brick or stones were reduced to a minimum at the times when the structures were experiencing minimal internal forces, allowing for the horizontal forces to cause relative horizontal displacements between the different masonry units.

The vertical acceleration components of earthquakes are often ignored or disregarded in current research and design of URM. As it will be shown later, vertical accelerations, especially in the higher frequency range and near the faults, can be larger than the horizontal accelerations. Therefore, the effect of the combination of both the horizontal *and* the vertical accelerations should be taken into account in URM studies.



(a)



(b)

Figure 1-6. (a) Stone masonry with thick joints; (b) partially damaged dome



(a)



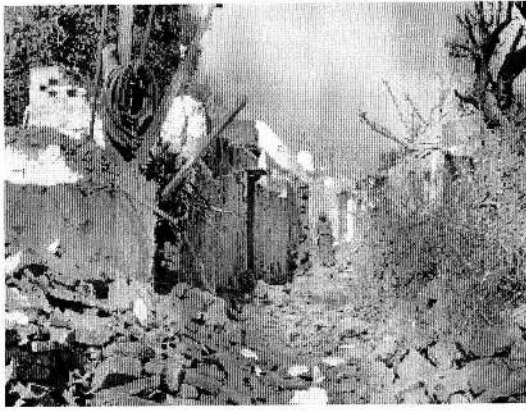
(b)

Figure 1-7. (a) Heavy roofs; (b) no roof-wall connections a common problem

1.4.3 Bhuj – India

The Bhuj earthquake occurred on January 26, 2001 and had a maximum intensity of Mw7.6. Over 350000 houses were fully destroyed and nearly one million damaged. About 50% of the population of 40 million in the Indian state of Gujarat was directly or indirectly affected by this disaster, which caused an excess of \$5 billion in damages (CIRES 2001).

The large majority of the damaged structures were either stone or brick masonry (Figure 1-8a) with deficient or no reinforcement. In some villages, up to 95% of the houses collapsed or were severely damaged as can be seen in Figure 1-8c. As was the case with Bam, Gujarat is a wealthy state with enough resources to build earthquake-proof housing. In spite of being wealthy, both reinforced and unreinforced structures were either poorly designed or built, resulting in their deficient seismic performance. It is worthwhile to note that the traditional locally built “Bungas” (Figure 1-8b), which are inhabited by the lower castes and poor, performed quite well. This good seismic performance was the result of their circular shape, which did not induce stress concentrations (Figure 1-8c).



(a)



(b)



(c)

Figure 1-8. (a) Damage to URM structures; (b) Bunga house; (c) Destroyed village (Photos: Eric Marti).

1.5 Discussion

An excess of *one billion* people live in over one hundred million houses that are not seismically safe in earthquake prone regions of the world (CHRR). Most of these houses are built with masonry units and have no or deficient reinforcement. The dynamic behavior of URM still remains to be accurately understood. The number of deficient, low-cost housing units is not about to decrease: “The overwhelming shelter problem in the developing countries is the shortage of affordable housing for the low-income majority of households in urban areas. This has resulted in the proliferation of slums and squatter settlements”(UN-Habitat 1999). The purpose of this research is to contribute to the better understanding of URM conducive to improved construction practices and retrofit schemes.

1.6 Thesis Outline

This thesis first describes why the enormous global need for improved URM construction and retrofit practices is the primary motivation for this research. Then, a literature review of the topics of particular interest for this research is conducted. To ensure that the reader will fully understand the issues discussed, background knowledge of the main concepts involved in the experiments and results is provided and the pros and cons of stone and brick masonry are presented. This is then followed by a detailed description of the experimental methodology used during this research. Next, the behavior and failure mechanisms observed during the static and dynamic experimental tests and the numerical models is analyzed and quantified, and a number of significant detrimental effects of the seismic high frequencies on unreinforced masonry are identified. Subsequently, a series of low-cost construction improvements and retrofit schemes are proposed and described based on the observations made during the experiments and recent earthquakes. Finally, the major conclusions are presented and the necessary future investigations to further describe and quantify the effect of high frequency / low-energy seismic waves are suggested.

Chapter 2

2. Literature Review

The first part of this chapter focuses on three major concepts that are at the core of a better understanding of this research, namely the effect of high frequencies on structures, the shear fluidization of granular soils and the soil-structure interaction in the case of retaining walls and silos. Then, a brief overview of the strengths and shortcomings of conventional methods for analyzing URM will be presented.

2.1 High Frequency Seismic Vibrations and Masonry Structures

The author has not been able to locate any scientific literature or research project directly studying the impact of high frequency seismic vibrations on URM structures. The absence of research in this field strongly suggests that high frequencies are not considered a threat to structures, due mainly to two arguments. First, frequencies beyond 15Hz do not resonate with the commonly built housing structures because they are higher than the structures' first natural frequencies. As a rule of thumb, the natural frequency of a building in Hz is equal to ten divided by the number of stories. This means that a ten-story building has a natural frequency of 1Hz and a one-story building 10Hz. Second, the energy content (which is proportional to the magnitude of the wave, Plate Tectonic 2005) of high frequency seismic vibrations is very low, resulting in their being disregarded as a potential source of structural damage.

Typical earthquakes show their highest energy contents at frequencies below 2-3Hz; the 1999 Bhuj earthquake had peak energy contents at frequencies around 2Hz, as can be seen in Figure 2-1 (dotted line), where the energy content at different vibration frequencies of the ground for two nuclear explosions can also be seen as a continuous line (Gupta et al., 1998). It is interesting to note that the ground vibration frequencies at which the energy content is highest in nuclear explosions occur between 4 – 6Hz. The total *seismic* energy released in an earthquake (which is not the *total* energy released) is the sum of the energy content of the two most significant seismic waves: P-waves and S-waves (which will be discussed later), containing approximately 5% and 95% of the total radiated energy, respectively (Xyoli 2002).

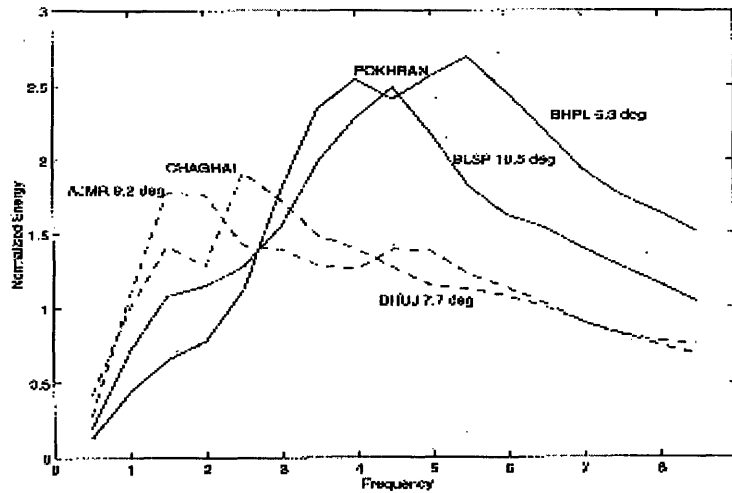


Figure 2-1. Comparison of spectral contents of Pokhran and Changhai explosions at similar epicentral distances (Gupta et al., 1998).

Existing literature concurs that the energy content of seismic waves with frequencies higher than 15Hz is much lower than at frequencies below 4Hz. However, the literature has only recently started to address the significance of the frequencies of the seismic waves' vertical component and how they could have a detrimental effect on structures.

“The vertical component of earthquake ground motion has generally been ignored in the seismic design of structures. However, this is gradually changing due to the increase in near-field records obtained especially in the last decade, and the field observations showing the possible damaging effect of strong vertical motions.” (Kambod et al. 2004)

During the 2003 earthquake in Bam the strong motion records showed that the maximum horizontal accelerations were between 0.7 and 0.8g, whereas the maximum vertical acceleration was about 1g (Kambod et al. 2004).

The evident effect of the vertical accelerations resulting from the vertical vibration component of seismic waves is that the structures' “self-weight” does not remain constant, but rather oscillates over time. This will result in increasing and decreasing internal stresses that, especially in the case of URM, affect the friction resistance between the different masonry units (stone or brick), which in turn will influence the overall stability of the structure. This is especially true in the case of dry stone masonry. Here the stability of the wall relies entirely on the frictional resistance holding the stones together, which could be dramatically reduced by vertical vibrations.

A more subtle effect of the vertical frequencies can be found on how these could affect the core granular material of a two-wythe wall. This phenomenon has not been directly studied in the URM context; however, studies have been conducted related to the resonance frequencies of vibrated granular soils with the intention of achieving a better compaction. As can be seen in Figure 2-2, dry granular soils show a resonance region between 12Hz and 20Hz, which will vary depending on the material properties and the overburden (Massarsch 2005). It is in the resonance domain that the shear fluidization of granular material will be most significant.

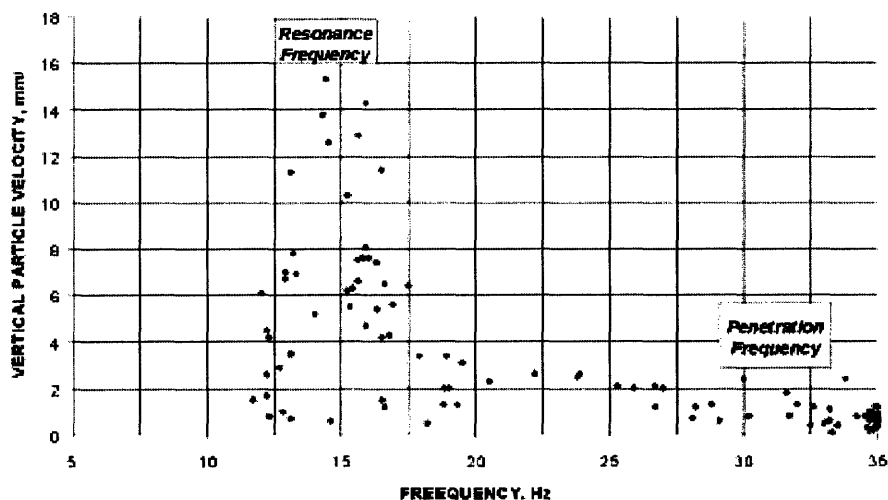


Figure 2-2. Vertical ground vibration velocity at a distance of 4 m from the compaction probe during probe penetration and resonance compaction (Source: Massarsch 2005).

2.2 Shear Fluidization of Granular Soils

The study of shear fluidification in geotechnical engineering has become broader in recent years, especially for earth-retaining structures. The U.S. Occupational Safety and Health Administration OSHA warns that “granular soils are susceptible to shock and/or vibration failure (OSHA 2004).” Richards et al. conducted extensive research on shear fluidization of soils, and found that when the fluidization occurs, “material behaves as a fictional fluid rather than yielding as a solid; it is as though the material had melted under stress” (Richards et al. 1990). Fluidization is used to describe the shear flow of material, which will increase as acceleration increases, and should not be confused with the fundamentally different liquefaction phenomenon. Moreover, fluidization can occur in granular soils with no pore

water, which is the case of interest for this research. In case of saturated loose soils, initial fluidization will most probably cause liquefaction of the soil (Kumar 2001).

The investigation of the exact mathematical formulation of the shear fluidization is beyond the scope of this paper; however, there are two important facts that are relevant to this research. First, it is the horizontal, rather than the vertical, component of the acceleration that will cause shear in the material and its fluidization. The vertical component can speed up the fluidization process by reducing the net inter-particle frictional forces. Second, the horizontal acceleration needed to initiate fluidification depends mainly on the type of soil and, to a lesser degree, on its density. Sandy, dense soils will start fluidizing at horizontal accelerations of 0.295g, whereas loose sand start fluidizing at 0.28g. The relevance of soil fluidization in this research is that it will result in an increase of outwards internal pressure on the wall wythes coming from granular infill materials. This phenomenon has not yet been investigated in the context of two-wythe unreinforced structures with granular infill, but has been extensively addressed in the context of retaining walls. Therefore, for the purpose of better understanding this phenomenon, the relevant literature on soil-structure interaction in retaining walls and silos will be briefly reviewed.

2.3 Granular Soil-Structure Interaction

2.3.1 Retaining Walls

The design and behavior of retaining walls has been studied extensively. This review will focus on the issue that is common to retaining walls and the wall specimens tested for this research: lateral pressure on the wall wythes resulting from granular infill. There are two limit states in lateral earth pressure acting on retaining wall, active and passive. At rest earth pressure occurs when the wall is restrained and cannot move laterally. Passive earth pressure develops when the pressures on the wall cause it to move into the soil. Finally, active earth pressure develops when the wall moves outward (Figure 2-3). It is the active earth pressure on a vertical cantilever retaining wall, which would be the non-arched, minimum tangential stress that is analogous to the two-wythe brick wall with granular infill.

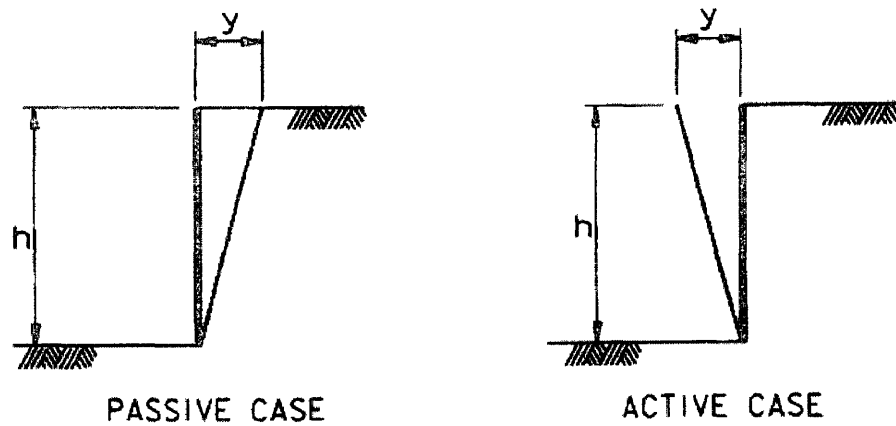


Figure 2-3. Passive and active earth pressures; h is the wall height; y is the wall displacement (US Army Corps of Engineers 2005).

The ratio of the horizontal and vertical stresses in homogeneous soils is given by the coefficient of earth pressure at rest, K_0 :

$$K_0 = \sigma_h' / \sigma_v' \text{ and also } K_0 = 1 - \sin \phi'$$

for consolidated clays and granular soils, where ϕ' is the friction angle of the material. From these two equations, given a vertical stress— $h \cdot (\text{soil density}) / \text{area}$ —and the friction angle of the material, the limit lateral stress can be found. The effective lateral stress will be smaller depending on the soil conditions. In the case of the masonry walls, the granular material is restrained by two wythes standing close together, which results in some of the weight of the infill material going into the wythes in the form of vertical shear forces, V_s , as seen in Figure 2-4. This transfer results in a non-linear increase of the lateral soil pressure q . This force setup will be used in the calculations of lateral infill pressures.

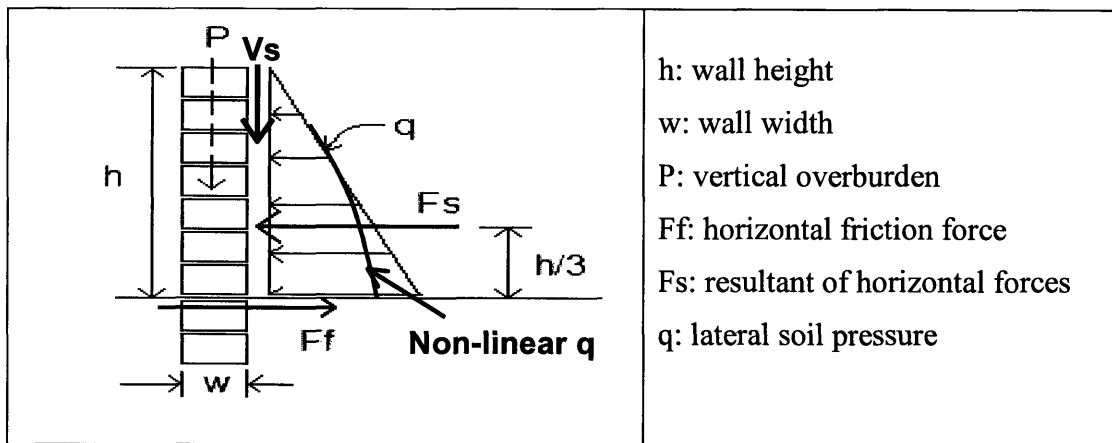


Figure 2-4. Free body diagram of the forces acting on a wall wythe, including the vertical shear (V_s) and non-linear lateral soil pressure.

2.3.2 Silos

From the outside, a silo may look very different from a masonry wall. However, the stresses generated by the stored granular material on the container walls show resemblance to those occurring in a retaining wall or a two-wythe brick masonry wall. In Figure 2-5 four cross-sectional cuts of a silo show the wall's normal stress, σ_w , and the different assumptions of what the trajectories of the principal stress could be (Schultze 2005). From these cross-sections it can be seen that the stress distribution in the vertical section of a silo is similar to the stresses in an infilled masonry wall. The research done on silos that is relevant to this study is the one concerned with the change in internal pressures caused by the vibration of the granular material.

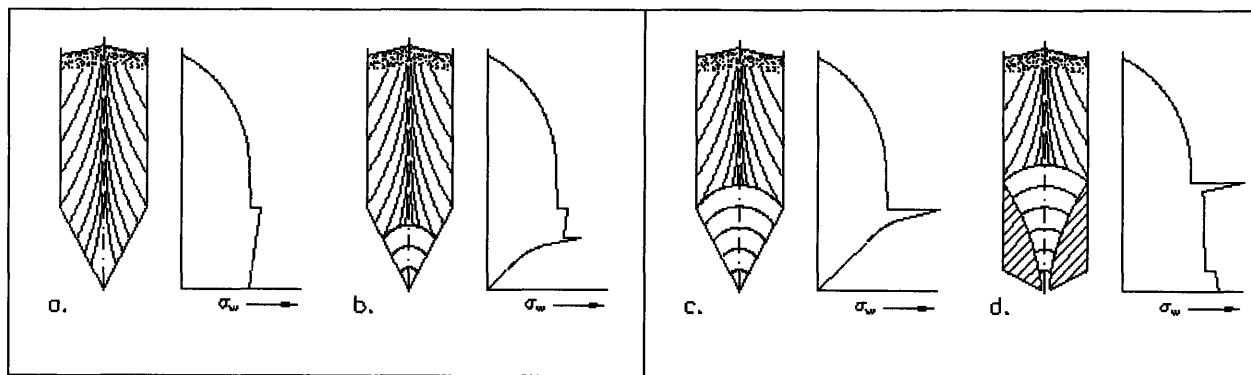


Figure 2-5. Qualitative courses of wall normal stresses, and assumed trajectories of the major principal stress (Source: Schultze 2005).

In the static case, the wall stresses in a brick wall with granular infill will be similar to those found in silos: simple non-linear increase with depth. The main difference is that the shape of the silo is pointed and the transition from the vertical wall to the slanted base can cause stress concentrations. No such stress concentrations caused by wall slanting will occur in a URM wall. In the dynamic case, the behavior of the granular infill, both in silos and URM walls, will be similar; however, the failure mechanisms will be significantly different, mainly due to the distinctive flow of material and stress concentrations in silos.

A number of catastrophic silo failures have been caused by flow-related dynamic load conditions that had not been taken into account during the design process (Carson 2005). Most of the failures are due to construction and design errors, and in a few cases due to silo usage and maintenance. In a number of cases it has been observed that the vibrations generated during the emptying of the silos can generate additional, unaccounted stresses that can lead to different degrees of failure (Carson 2005). In the case of URM walls, the granular infill during a seismic event can also generate additional wall stresses if the vibration frequency is close to the resonant frequency of the infill. None of the existing methods to analyze URM take into account the possible stone ratcheting and shear fluidization of the infill.

2.4 Conventional Methods to Analyze URM

There are four main methods to analyze URM structures: the traditional finite elements, the discrete elements, the use of distinct panels to describe the structure, and the probabilistic risk assessment.

2.4.1 Finite Elements Method: FEM

Originally, the FEM method was developed for homogenous and isotropic materials, where the overall behavior of the structure is based on the material properties. This continuous system approach works well for steel structures and, to a lesser degree, for reinforced structures where no material degradation is expected. Because of the user-friendliness and attractive output, FEM has often been used to analyze non-homogenous and anisotropic URM structures (and their retrofit schemes). In recent years, the FEM method has been improved by introducing non-linear material behavior and the (limited) capacity to model crack initiation

and propagation. However, it is still far from fully capturing the behavior of URM structures, especially under dynamic loading. Numerical modeling of URM structures using FEM is computationally very expensive because their typological characteristics cannot be simplified and the mechanical properties lead to significant non-linearities (Giordano et al. 2005). Three significant URM structural properties that are yet to be resolved in the FEM software are inherent absence of tensile strength, degrading of the material, and failure initiation and propagation.

Recent improvements in FEM modeling include two new models: the “two-material model” and the “equivalent-material model.” The two-material model separates the individual masonry units by joint (mortar) elements, where the discretization matches the patterns in the masonry structures. The main disadvantage of this model is that it quickly becomes computationally very expensive because of the large number of elements needed to represent the simplest structure (Giordano et al. 2005). However, the two-material model can be used to analyze parts of the structure that are of special interest when a detailed analysis is required.

The equivalent-material model analyzes masonry as a homogeneous continuum that will be meshed and will provide a constitutive model exhibiting the average behavior of the structure. This model does not directly represent the actual URM structure, but is able to grasp a number of significant trends in its behavior, with a much reduced computational cost compared to the two-material model.

Neither of the two previously described FEM models is able to provide as satisfactory results, when it comes to the failure initiation and propagation in URM, as the discrete element method (DEM), which is a discontinuum analysis technique.

2.4.2 Discrete Elements Method: DEM

The discrete elements method (DEM) was initially developed to model the behavior of cracked rock masses in geotechnical engineering. Some of the strongest capabilities of DEM are its suitability for modeling crack initiation and propagation, as well as large displacements between the different masonry units (Azevedo et al., 2005).

In DEM the structure is divided into a number of distinct blocks that can either be rigid or deformable. The interface between the different block units is based on a series of elasto-

plastic point contacts, which allow for contiguous blocks to be connected along these points where the shear and normal forces are resolved (Giordano et al. 2005). Unlike in FEM, where the contacts are fixed, in DEM the blocks can lose existing contacts and make new ones, allowing for large relative displacements between blocks (Figure 2-6) typical of URM (Azevedo et al. 2005). In this research a DEM software (UDEC) will be used as the modeling tool to analyze the static and dynamic behavior of two-wythe, infilled brick masonry walls.

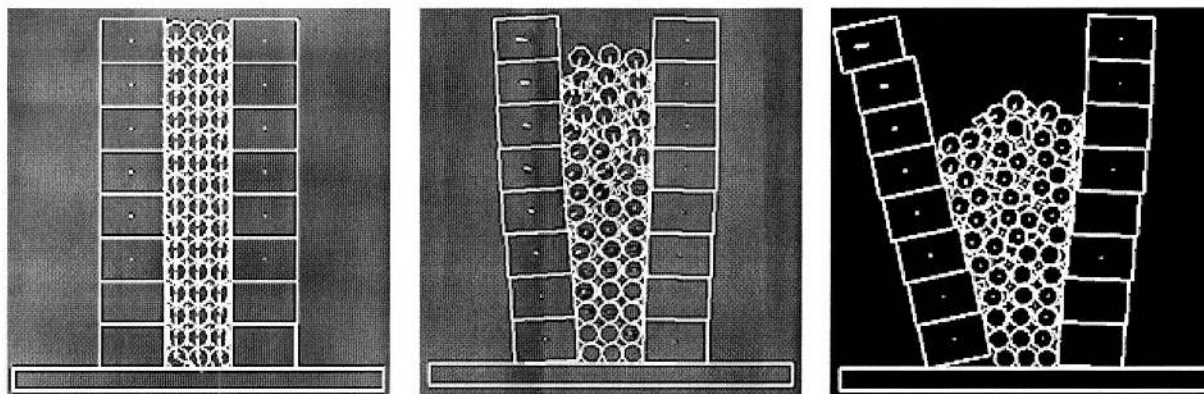


Figure 2-6. An example of a DEM where both the wall units and the infill are modeled with discrete elements.

2.4.3 Distinct Panels

The distinct panels modeling method combines FEM and DEM to analyze large structures efficiently. It divides structures into a number of sections based on the structure's skeleton, openings, and expected failure mechanisms. This method allows for a significant reduction of computation time while focusing on the most probable failure mechanisms. It is like DEM, but with much larger homogeneous blocks.

A. Penna (2004) developed a 3D-masonry model where, by means of internal variables, the macro-element or panel considers both shear-sliding damage and its evolution, and rocking mechanisms, which have a toe-crushing-effect. This is achieved by dividing the macro-element into three parts: two layers, inferior and superior, in which the bending and axial effects are concentrated, and the central part, which undergoes shear-deformations only. The kinematics is described by an-eight-degree of freedom vector for each macro-element. The panel shear response is expressed by considering a uniform shear deformation distribution, with cracking damage usually located on the diagonal when Coulomb's limit

friction condition is reached. Toe crushing is modeled by means of the “phenomenological non-linear constitutive law with stiffness deterioration in compression” (Penna 2004). Further, each wall of the building is subdivided into piers and lintels connected by rigid areas, which are not representative of URM. This model is good for RC structures with masonry infill, homogeneous materials, and symmetric dimensions. However, it is not useful when masonry irregularities control the failure, which is the case in the majority of URM structures, where they are the reasons the failures are initiated and propagated.

Felice (2004) has developed an interesting model to assess the out-of-plane fragility of masonry walls. In his model he defines the three factors responsible for the out-of-plane resistance of masonry as mortar’s tensile strength, the interlocking pattern of masonry units, and the size of the masonry units. The out-of-plane capacity decreases with decreasing interlocking of the masonry units. A factor λ is introduced to account for the internal slenderness of the wall, which is the width-to-height ratio of the unrestrained face of the wall. Among all the investigated methods, this is the only one that considers delamination as one of the possible failure mechanisms.

2.4.4 Probabilistic Risk Assessment

The purpose of the probabilistic risk assessment method is to estimate building stock loss at the urban or regional scale, based on displacement/drift demand (Velez 2003). In this method the in-plane demand is represented by the displacement response spectrum obtained from regional probabilistic seismic hazard studies. For the out-of-plane mechanisms, the procedure is restricted to simple one-way bending mechanisms. To do seismic risk estimation at regional scale, risk assessment of classes of buildings is used. This method is an efficient tool to assess the overall seismic safety of entire towns or regions, but should not be used to analyze individual structures.

D'Ayala and Kansal (2004) present another interesting methodology to categorize a large number of buildings by identifying a number of failure mechanisms and structural deficiencies, after which she proposes a series of strengthening measures. The aim of this method is to identify specific construction techniques and assemblies that have shown particularly high vulnerability and assess whether the given typology is common in the

region, using a numerical assessment procedure. Four typologies of masonry are considered, depending on the degree of their structural integrity:

A1 - Solid squared masonry with sufficient connection

A2 - Three-leaf solid masonry with insufficient level of connection in the wall thickness

B - Mixed masonry made of squared stones and sun dried-bricks

C - Rubble masonry with insufficient connection

Some of the parameters included in the method are: geometric data, building configuration, typology of vertical and horizontal structures, structural integrity of masonry walls, corner connections between two orthogonal walls, and size and placement of openings. These parameters are representative of masonry structures, but do not include two major factors: foundations and soil conditions.

2.5 Discussion

The literature review of high frequency seismic vibrations has shown that, in spite of their being far from the natural frequencies of typical structures, they can be the trigger to initiate structural failure of URM and cause the shear fluidization of a granular medium. Shear fluidization is a familiar term in geotechnical engineering; however, it should also be taken into consideration in studies of the dynamic behavior of URM structures, where it can cause crumbling of dry stone walls and a increased core material wall pressures. In the present research, and due to a lack of literature related to these two significant phenomena, literature related to retaining walls and silos was used to predict their impact on masonry structures. Different numerical models—FEM, DEM, Distinct Panels, and Probabilistic Risk Assessment—were explored to identify the most suitable to analyze URM under dynamic loading. DEM was chosen because it allows for the modeling of material shear fluidization, the inter-stone vibrations, and large relative displacements. These omissions could, as we shall see, distort the model's behavior and lead to dangerous assumptions about real structures.

Chapter 3

3. Background Information and Theory

The background information provided in this chapter will help the reader become familiar with the material and structural properties of unreinforced stone and brick masonry. Relevant information about seismic waves, frequencies, shear fluidization and ratcheting, compaction, and arching effect will also be provided. This background will put the research into the appropriate framework and provide the reader with the necessary tools to understand the arguments used to set up the experiments and draw the conclusions from the results.

3.1 Unreinforced Stone Masonry (URSM): Advantages and Disadvantages

Proper construction of unreinforced stone masonry (URSM) structures requires good skills and awareness of its inherent weaknesses and the hazards that it could pose, especially in the case where the structure has to resist seismic loadings. There are a number of advantages and disadvantages of this construction material.

3.1.1 Advantages

Cost. In most rural areas where stones are to be found they are available at no other cost than labor. This makes them an extremely attractive construction material for a population living in poverty.

Availability. Stones are available in sizes that can be easily handled without any specialized equipment. Stones can be directly used as construction material without any intermediate process other than having to shape them to improve the way they fit together.

Familiarity. Construction using stones in regions where stones are readily available is often the traditional way of building houses and other structures. Therefore, the skills needed for construction are available locally and are passed down from one generation to the next. However, this familiarity with the traditional construction skills is being lost in recent years for two main reasons. First, the younger generation no longer takes the time to carefully learn from their elders, concentrating instead on building a shelter as rapidly as possible. The construction increasingly involves the amalgamation of different unfamiliar materials and techniques. Second, an increased interregional migration, motivated by better economic prospects, brings people to

regions where they are unfamiliar with the local hazards (e.g., seismic/non-seismic, flooding) and construction practices. This unfamiliarity, added to the time pressure to make a stable shelter, often result in deficient constructions.

Material properties. The compressive strength of stone itself is never a limiting factor in the construction of residential dwellings. In addition, stone is the most durable construction material and provides a good finished appearance.

3.1.2 Disadvantages

Tensile strength. The main disadvantage of stone masonry is that it has zero or near-zero tensile strength. This is not a problem in the static condition. However, under dynamic loading, URSM's lack of tensile strength and minimal toughness become an almost insurmountable problem.

Weight. The use of stone in construction results in very heavy structures. This large weight can be very detrimental under seismic loading, where the induced lateral forces that the structure has to carry increase linearly with the weight. In addition, a collapsing stone house will often result in severe injury or death for its occupants and people nearby.

Image. Stone masonry is regarded in many developing countries as “the masonry of the poor,” making it unattractive to its dwellers. Those who can afford to will plaster the wall surface, hiding the raw construction and making it difficult to assess the structural integrity of the house.

3.2 Unreinforced Brick Masonry (URBM): Advantages and Disadvantages

3.2.1 Advantages

Availability. Thanks to transportability, fired bricks are readily available almost everywhere and are relatively cheap.

Constructibility. The uniform shape of the brick units greatly facilitates the construction process and facilitates the dimensioning of the house partitions and openings. In addition, the bricks can be shaped in such a way as to allow reinforcement to run through them, becoming, if designed properly, a well-performing structure under seismic loading.

Appearance. The finished look of bricks is more acceptable than stone to low-income families.

3.2.2 Disadvantages

Tensile strength. As with stone masonry, URBM has little tensile capacity. However, its density is lower than stone and the material used for a construction of the same occupancy dimensions is much less; walls built with bricks turn out to be half as thick as stone walls. This results in a significant reduction of the overall weight of the structure and a proportional reduction in the shear forces (source of tensile stresses) in the walls.

Environmental impact. Two of the major environmental disadvantages of using bricks as a construction material are topsoil removal and deforestation.

Topsoil removal is an insufficiently studied side effect of brick masonry. In China, seven percent of the agricultural land has been lost to brick production. The problem of topsoil removal in Bangladesh has not been investigated in detail, however, farmers are often tempted to sell a thin layer of top soil for a quick gain, which results in a sharp drop in their agricultural production potential (Gomes and Hossain 2003). By first removing the organic top layer of the soil and then using the soil layer containing the appropriate grain distribution (with a depth ranging from less than one meter to dozens of meters), entire areas have been left infertile. In addition, the ditches left after removing the soil are often filled with trash and unhygienic water, turning into malarial mosquito breeding grounds.

Deforestation is a chronic problem in developing countries where energy is scarce. The firing of bricks needs large amounts of wood or charcoal, straining the already scarce fuel supply. Besides other deterioration of the environment caused by deforestation, it also greatly increases the risk of landslides, which in recent years have been increasing in number.

Durability. Depending on the brick quality, the exposed bricks may degrade quickly under harsh weather conditions, reducing the durability of the overall structure.

3.3 Seismic Waves

Earthquakes occur when two or more tectonic plates abruptly move with respect to each other to release shear stresses that have accumulated. The rough rocks of the adjacent plate surfaces rubbing against each other generate seismic waves. The four main types of seismic waves generated in this process are shown in Figure 3-1. P-waves vibrate only horizontally in the direction of propagation in the form of shock pulses. S-waves and Rayleigh-waves can be

compared to sea waves and have a vertical motion component, resulting in horizontal as well as vertical accelerations. Finally, Love waves vibrate horizontally and perpendicular to the direction of wave propagation. The relationships between the different parameters that define a wave – wavelength, frequency, period-- are shown in Figure 3-2.

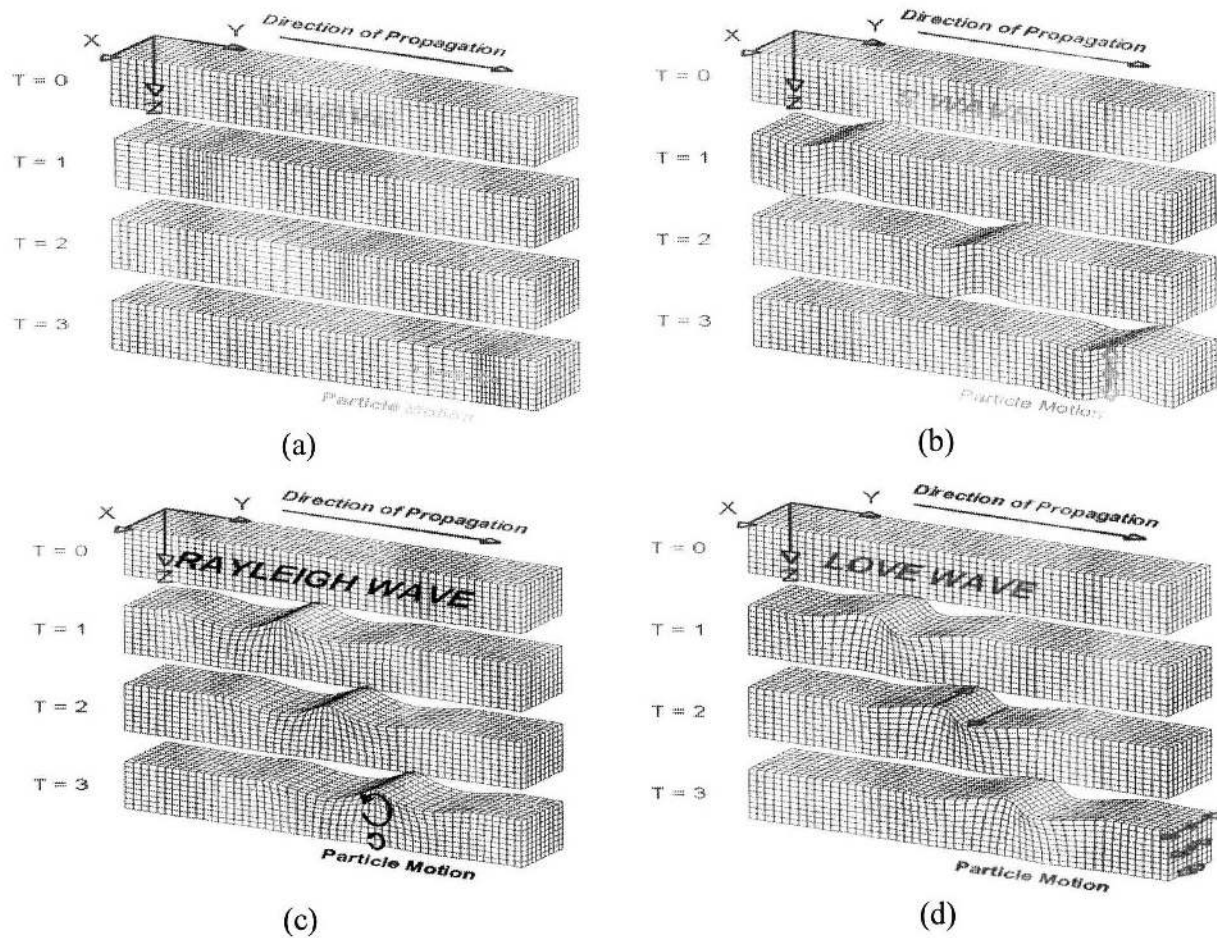


Figure 3-1. The four main types of seismic waves: (a) P-wave; (b) S-wave; (c) Rayleigh wave; (d) love wave (Braille).

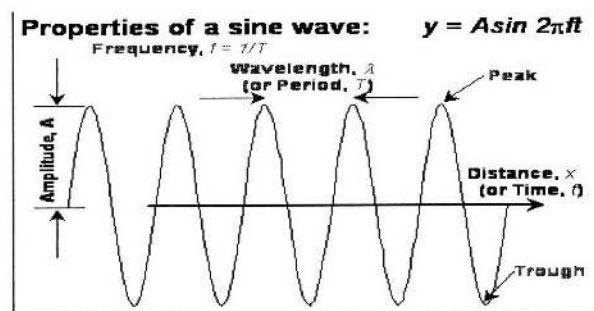


Figure 3-2. Parameters defining the properties of a wave (Braille).

Traditionally, only the horizontal vibration component of a seismic wave is taken into account to estimate the loads that a structure will experience from an earthquake. However, the vertical component of the wave motion can contribute sometimes as much, if not more, to the structural damage as the horizontal component. The vertical motion component of the seismic waves is most significant near the epicenter (near-fault effect, Stewart 2001) and at frequencies of 10Hz and higher, which are the frequencies that this research is concerned with (Singh 2005). Hence, the maximum accelerations experienced during an earthquake can occur at frequencies higher than 10Hz, currently disregarded as being too high to cause any damage. In addition, vertical vibrations/accelerations have only recently been scrutinized as a potential source of structural damage: “The vertical component of earthquake ground motion has generally been ignored in the seismic design of structures. However, ... field observations show[ing] the possible damaging effect of strong vertical motions.” Vibration frequencies higher than 10Hz have been fully ignored with regards to structural damage in buildings. Their impact on structures will be reviewed next.

3.4 Frequencies

Generally, frequencies beyond 10Hz are not taken into consideration as a source of possible structural damage. Two valid arguments used to disregard them are, first, the fact that the vast majority of natural frequencies of structures are lower than 10Hz (the first mode of an one-story URM structure can occur at a frequency higher than 10Hz) and, second, that the energy content of higher frequency vibrations is very low. These two explanations are valid if the structural failure mechanisms considered are excessive lateral displacements and rocking of the structure. However, in the case of URM there are at least two failure mechanisms that can be triggered by high frequency / low energy seismic waves: crumbling and wall deformation resulting from the shear fluidization of the wall's inner core granular materials. It is the brittle nature of URM that makes it sensitive to high frequencies (Stewart 2001). Hence, there is a need to better understand how high frequency vibrations propagate and what their relative significance during a seismic event is.

Seismic high frequencies have been studied extensively in geology, however, not so in structural engineering. Eiichi Fukuyama and Raul Madariaga have demonstrated “a rupture front focusing phenomenon at the initial stage of earthquake, which causes high slip rate pulses and

therefore generates high frequency seismic waves” (Fukuyama and Madariaga 1999). High frequencies dissipate quickly in soft soil and propagate further in stiff soils or rocky terrain. Furthermore, tests conducted by Mark Svinkin show that the range of dominant frequencies of waves propagating from blasting in construction sites and quarries (which is similar to what occurs in an earthquake with the sudden release of energy) mainly range between 10 and 60 Hz. These results show that high frequency vibrations are significant during earthquakes and, as will be shown later, they can be detrimental to brittle structures. Moreover, it is the high frequency vibrations that are at the source of the shear fluidization and ratcheting of granular soils (Svinkin 1999).

3.5 Shear Fluidization and Ratcheting

Shear fluidization and the resulting ratcheting, are familiar terms in geotechnical engineering and have been linked to the failure of granular soils (Gudehus 2003). However, the phenomenon of shear fluidization has not been investigated in the context of URM, where the structure itself, or its components, can behave like a granular soil. In granular soils shear fluidization results from a loss of inter-particle shear forces due to vibrations traveling through the granular medium. This reduction in shear forces alters the overall behavior of the soil, making it behave more as a fluid-like material and initiating stepwise accumulation of small relative displacements between the particles, known as ratcheting. Shear fluidization and ratcheting can develop between the stone units and in the granular infill (Marroquin and Herrmann 2003).

The small displacements caused by ratcheting accumulate and could ultimately result in large enough wall deformations to cause its crumbling. In addition, shear fluidization affects the granular infill common in thick walls of ancient buildings. During the shear fluidization of the granular infill, its angle of repose is significantly reduced. When the granular soil is constrained laterally, as is the case in two-wythe masonry walls with a granular core infill (Figure 1-2), the reduction in angle of repose causes an *increase* of the internal horizontal pressure against the wythes (Richards 1990). It is this increase in internal horizontal pressure that contributes to the deformation of the wall and, ultimately, exacerbate its crumbling. This phenomenon has been extensively studied in the context of silos.

Vibration experiments conducted by Maciej Niedostatkiwicz, (e-mail communication) in thin, tall silos show that the resonance (mass flow) for granular material similar to sand was

45Hz at the beginning of the silo emptying process. The resonance frequency decreases with increasing silo size. For large silos the resonance frequencies are much smaller, in the range of 8-10Hz. Besides the silo size, it is the stiffness of the granular material and the geometric and material properties of the container that will have the greatest effect on the resonance frequency of the system. The resonance frequencies depend to a lesser extent on the size of the granular material; it was found that sand and gravel would resonate at similar frequencies (Niedostatkiewicz 2005).

Finally, Niedostatkiewicz found that in large silos the standard increase of wall pressure during emptying is about 30-40%, which in the past has burst some silos. Moreover, in laboratory tests on silos, he observed a 200-300% increase of wall pressure during resonance. These results confirm that the increase in internal pressure that an infilled two-wythe wall, which has a number of structural similarities to a silo, could experience an increase in internal horizontal stresses resulting from the dynamic loading significant enough to cause structural damage. Shear fluidization and ratcheting are both conducive to the compaction of granular soils.

3.6 Compaction of Dry Granular Soils

Compaction of dry granular soils consists in reducing the volume of air in the soils (Figure 3-3a) and results in an increased soil density; vibration is the most effective way to compact them (Soil Compaction Handbook 2005). Traditionally, soils are compacted to increase their strength and prevent their liquefaction (if water is present) and unwanted excessive settlement. Extensive studies and information are available describing the different compaction methods. However, not much is known about the process that the soil particles undergo during the compaction process. A compaction criterion of granular soils is based on vibration frequency and velocity (Massarsch 2005). From Figure 3-3b and assumed or measured values of the "elastic" shear wave velocity through the medium, it is possible to relate ground vibration levels to the densification process. Moreover, permanent soil compaction can be expected when sandy soil undergoes multiple vibration cycles with strain levels above 12% (Massarsch 2005).

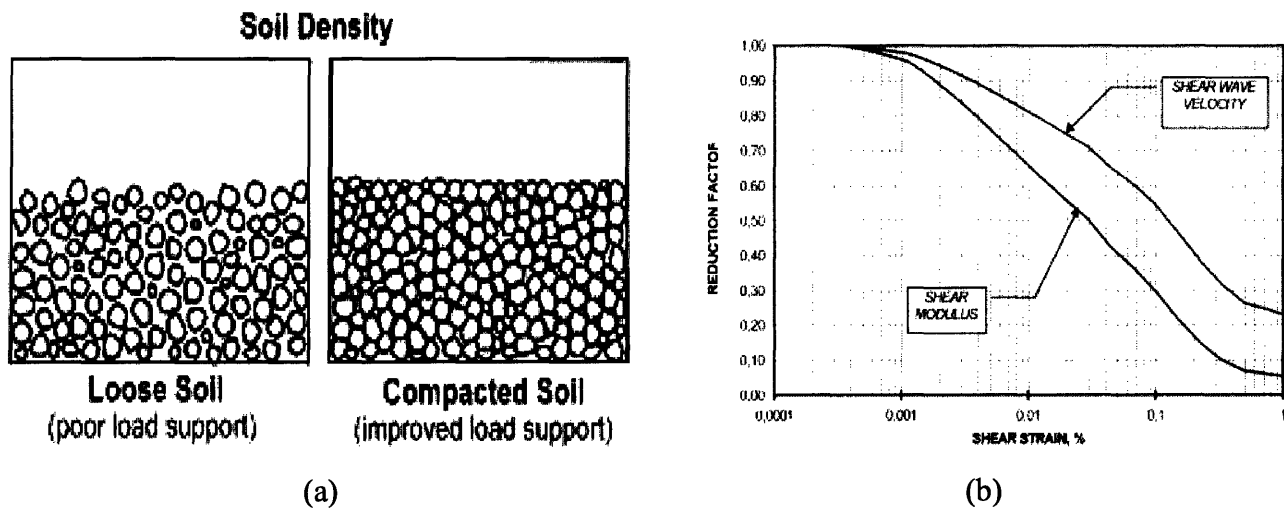


Figure 3-3. (a) Comparative drawings of loose and compacted soils; (b) Reduction of shear modulus and shear wave velocity as a function of shear strain (Rainer Massarsch)

A detailed study of how and why dry granular soils compact is beyond the scope of this investigation. However, during the compaction of dry core granular material in a stone masonry wall, an arching phenomenon can occur, resulting in significant changes in the horizontal thrust forces originating from the infill.

3.7 Arching Phenomenon

The arching phenomenon occurs when the particles of granular soils arrange themselves in arch-like structures that will transfer some of the soil weight into the wall (Keppler). Arching is a common occurrence during the discharge of containers of granular materials like silos, where the internal stresses will cause the grains to transfer the forces along arch-shaped paths (Figure 3-4). This change in load-path can result in a significant change in lateral stresses.

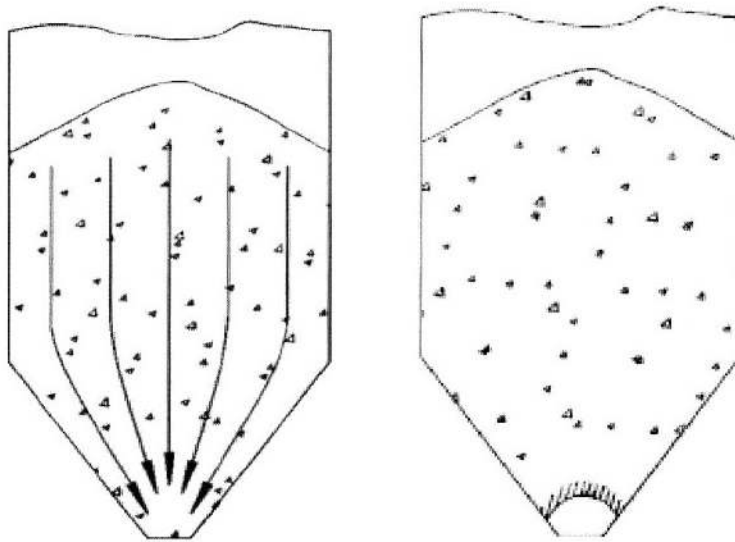


Figure 3-4. Grains in silos: natural mass flow and arching, (Schulze).

Commonly, the core of wide, two-wythe stone walls is filled in with rubble (granular soil), that over time will settle and will arrange itself in such a way to result in the arching of some of its particles and a reduction of the horizontal thrust. The diminution vertical stresses (and the consequent reduction in horizontal stresses) cause by granular arching was first studied by Jansse as early as in 1895, and was later called the Janssen's Theory (Take and Valsangkar 2001). The reduction in vertical stresses results from the transfer into the wall of some of the horizontal stresses as vertical shear stresses. In static conditions the arching effect will increase the overall stability of the wall by increasing the magnitude of the vertical forces in the wythes, while decreasing the horizontal overturning stresses. However, the arching effect will dissipate as soon as the wall experiences high frequency vibration, reducing the stability of the wall and increasing the outwards overturning stresses acting on it.

3.8 Discussion

The background information provided in this chapter shows that unreinforced stone and brick masonry structures are attractive to people with low incomes because of the availability of the materials and their reduced cost. The skills needed for these types of constructions are minimal and are traditionally learned within the community. It has been established that the limited shear resistance of URM makes it very susceptible to damage when loaded dynamically. Therefore, the different seismic waves have been illustrated and their probable damaging impact on URM

structures described. Furthermore, the literature shows how shear fluidization, induced by high frequency vibrations, can cause material ratcheting. Ratcheting, which results in cumulative relative displacements between the stone units that make up a stone wall, can ultimately cause wall crumbling. Finally, the literature also shows that high frequency vibrations can lead to the compaction of granular soils and the diffusion of the arching phenomenon. This background information will be used in the next two chapters: test methodology and analysis of results.

Chapter 4

4. Methodology

4.1 Preliminary Evaluation

A number of different methods have been developed to evaluate the in-plane shear capacity and out-of-plane behavior of unreinforced brick masonry. These methods, however, only consider the two most common failure mechanisms occurring in brick masonry structures: shear and overturning failure. Therefore, they cannot be implemented to study the behavior of stone walls, where wall delamination and crumbling are two significant failure mechanisms, or of two-wythe, infilled brick walls, where infill pressures can contribute to the wall failure. Moreover, the traditional methods consider structural collapse as a consequence of relatively large structural displacements and do not take into consideration failures generated by high frequency vibrations, where displacements for each vibration cycle are minimal.

Because the failure mechanisms of interest to this research are closely related to geotechnical phenomena, it was decided to use the model for retaining walls of narrow backfill width by Take and Valsangkar (2001) to calculate the pressures resulting from the granular fill acting on the interior of the two wythes of the walls. This model includes the reduction of horizontal stresses caused by the arching effect and is the most appropriate way to predict and investigate the forces generated by the wall infill. In Figure 4-1 the non-linear increase of the horizontal pressure with increasing depth is plotted for a granular material (coal) with a density of 8.1 kN/m^3 and a friction angle of 40 degrees.

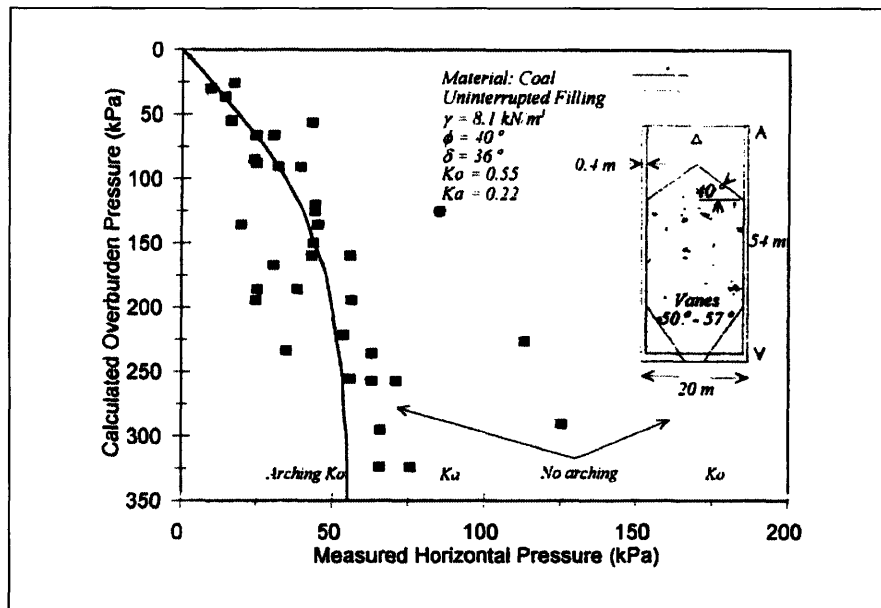


Figure 4-1. Horizontal pressures experienced by a retaining wall taking into account the arching effect (Source: Take and Valsangkar 2001).

The properties of the granular materials used as infill in the experimental tests of the brick walls are listed in Table 4-1. The different parameters used in the preliminary stress calculations to predict the failure mechanism of the brick walls are the following. The vertical shear coefficient ($K_v = 0.1$) acting on the interior of the wythes is based on values obtained from the US Army Corps of Engineers (1994). The coefficient of horizontal earth pressure at rest ($K_o = 0.5$) was obtained from the formula $K_o = (1 - \sin \beta)$, where $\beta = 31^\circ$ is the smallest friction angle of cohesionless soils used in the tests. The coefficient of static friction for the brick-brick interface was experimentally found to be 0.65.

Table 4-1. Physical properties of the different granular materials used as infill for the brick walls.

Material	Grain Size mm	Friction Angle β	Angularity
Fine Sand	0.5	31	Rounded
Gravel	15	34	Subangular
Coarse Gravel	60	38	Angular

To predict the failure mechanism and critical failure height of the walls, the horizontal inter-brick frictional forces (self-weight multiplied by coefficient of friction) and the lateral resultant forces, from the infill pressure for infill material with $\beta = 31^\circ$ on the wall versus increasing wall heights, are found and plotted in Figure 4-2a. From this plot, it can be

observed that the resultant force of the internal pressure (solid line) remains smaller than the resisting frictional forces (discontinuous line) beyond a height of 100cm, and therefore sliding failure will not occur. In Figure 4-2b, the overturning moments caused by the pressure acting on the wall (solid line) and the resisting moment, resulting from the self-weight of the wythe and the shear forces transferred into the wythes from the granular infill (discontinuous line) are again plotted versus increasing wall heights. This plot shows that the critical wall height needed for the soil pressure to cause overturning failure of the wythes is 60cm. From these two plots it can be concluded that the static failure mode would be by overturning at a height of about 60cm. This height was then used as a reference to build the first walls. The static failure height of the walls will vary, depending on the friction angle of granular material used as infill.

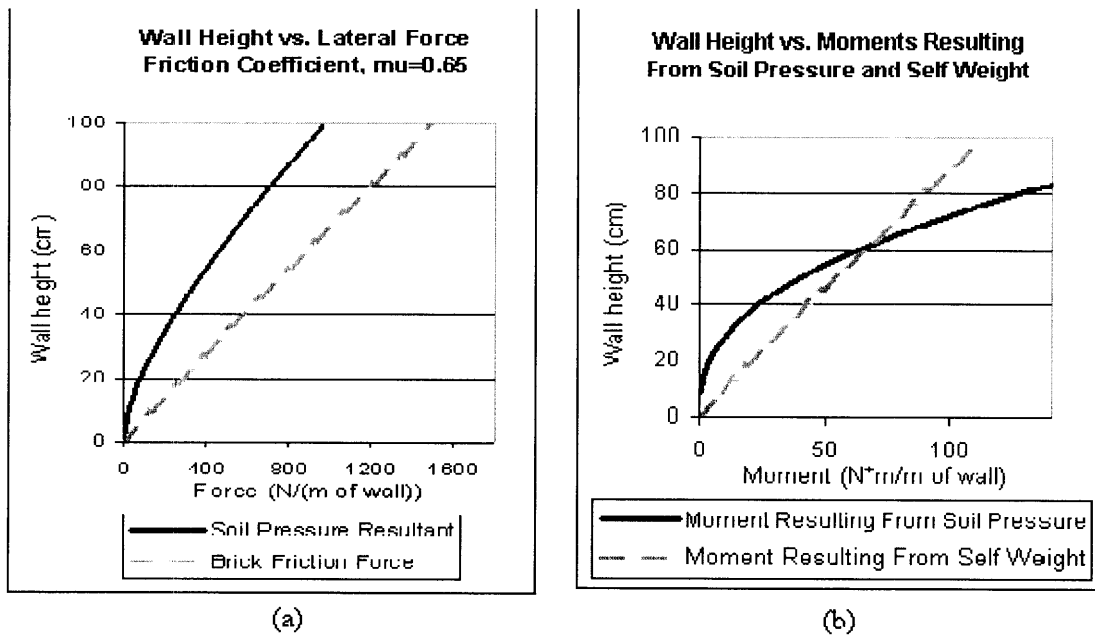


Figure 4-2. a) Wall height needed for sliding failure. b) Wall height needed for overturning failure, showing that a minimum wall height of 60cm is needed to cause overturning.

The prediction of the brick wall failure height under dynamic loading was difficult to make, because there is no previous research available on the effect of granular infill on masonry walls. Therefore, results from silo studies were used to approximate the changes in internal stresses due to high frequency vibrations. The two major wall stress modifications

were made to include the expected changes. First, the shear forces that were generated between the wall and the granular material in the static case will be dissipated when the infill is vibrated. Hence, there will be an increase in horizontal stresses on the wythes and a reduction of the forces resisting their overturning. Second, the vibrations will cause the granular infill to fluidize, resulting again in an increase of the horizontal pressure acting on the wythes. For these two reasons the dynamic failure height was predicted to be at least 20% lower than the static. In addition, it is important to note that the failure mechanism could change from overturning to sliding failure if a large enough vertical acceleration were applied to the wall. The vertical acceleration would linearly reduce the frictional resisting forces acting on the faces of the brick, hence reducing the overall resistance to sliding failure.

No preliminary calculations were conducted to predict the failure height of the stone specimens because, in this case, the overall dimensions of the walls were not considered a determinant factor. However, the stone walls were considered to be a granular material made up of large particles and they were expected to behave as such. As seen in Chapter 3, the range of resonance frequencies of granular media starts at about 12Hz and therefore, inter-stone vibrations were expected to become significant around this frequency, resulting in the crumbling failure of the stone wall.

4.2 Static Tests: Brick Walls

The purpose of the static tests was to find the wall heights at which failure occurs due only to the lateral pressure from granular infill materials with different friction angles. A standard wall base length of 38cm and width of 27cm were used, and the failure height varied depending on the infill friction angle. Cape Cod solid bricks (19.5x9x5.5cm) were used to build the walls, with the lateral boundaries between the two wythes made of cardboard or wood. The three types of granular infill had friction angles of 31°, 34°, and 38°.

For the static tests, the walls were built row-by-row and simultaneously filled in, until failure occurred. Numbering the bricks ensured consistency among the different walls. As anticipated by the preliminary calculations, the walls failed at heights that ranged from 48cm to 58cm, depending on the infill friction angle. That the experimental failure height was

consistently lower than the predicted one can be attributed to the irregularities in the shape of the bricks, which lowered the overall stability of the walls, especially the ones constructed in the earlier stages. Once the construction deficiencies were corrected, the failure height ranged from 54cm to 58cm. Furthermore, all the walls failed by overturning, as expected from the preliminary evaluations. No tests were conducted to find the static failure height of the stone walls because of the greater static stability of the stone walls.

4.3 Dynamic Test: Brick and Stone Walls

The brick walls used in the dynamic tests were identical to the ones used in the static tests, except that the heights were significantly reduced. The stone walls were built with irregularly shaped stones to a height of 45cm. Numbering the individual stones (Figure 4-3b) ensured wall consistency. The dynamic testing program consisted of two distinct testing phases: vertical and horizontal vibrations.

4.3.1 Vertical Vibrations

The first phase consisted of testing the walls dynamically on a vertically vibrating table with a fixed frequency of 60Hz and variable acceleration. This frequency is higher than the critical 15-25Hz resonant frequencies for granular soils (Massarsch 2005), which would result in the maximum infill lateral pressure. However, by varying the vertical acceleration, we were able to change the vibration intensity, and thereby investigate two significant dynamic behaviors of unreinforced brick and stone walls. First, we evaluated the effect of the increase of internal pressure on the two-wythe brick walls, resulting from infill densification and shear fluidization by vertical vibrations. The lateral forces resulting from internal pressures are particularly relevant in very old and historic buildings where the unusually wide two-wythe walls are infilled with rubble. Second, the effect of high vibration frequencies on dry, undressed stone masonry, commonly used in low-cost housing, was investigated. The testing procedure on the vertical vibrating table consisted in gradually increasing the vibration magnitude (i.e., acceleration) until failure. Video recording of all the tests allowed for time logging.

4.3.2 Horizontal Vibrations

In the second phase, the dynamic tests were conducted on a shake table with one horizontal degree of freedom. As seismic waves always have vertical and horizontal components, both brick (Figure 4-3a) and stone (Figure 4-3b) walls were tested under horizontal vibration to complement the previously conducted vertical vibrations tests. The walls were set up on the shake table in such a way that the motion would be applied along the plane of the walls. This setup was used to isolate the effect on the wythes of the shear fluidization and densification of the infill due to vibrations. If the vibrations had been induced perpendicular to the wall plane, two additional overturning forces would have resulted from the dynamic loading: the inertial forces of the wythes and the infill. The characteristics of the brick walls built on the shake table were kept the same as the ones tested statically, except for the slight increase of the brick width. This similarity allowed us to compare the static and dynamic failure mechanisms and properties.

Two testing procedures were used. The first consisted of inducing a sinusoidal vibration with variable frequency and a fixed maximum displacement. The wall was vibrated for two minutes at a fixed frequency and the displacement was gradually increased to the maximum desired. Then the vibration frequency was increased and held again for two minutes, while the vibration displacement was gradually increased to the desired maximum. This step-wise increase of frequency was repeated until the wall failed, which allowed us to identify the frequency and acceleration at which the walls started to fail and fully failed. These frequencies were then used in the second testing procedure, where the acceleration was gradually increased while the frequency was kept constant. These tests allowed us to confirm that high frequency / low energy vibrations could induce failure.

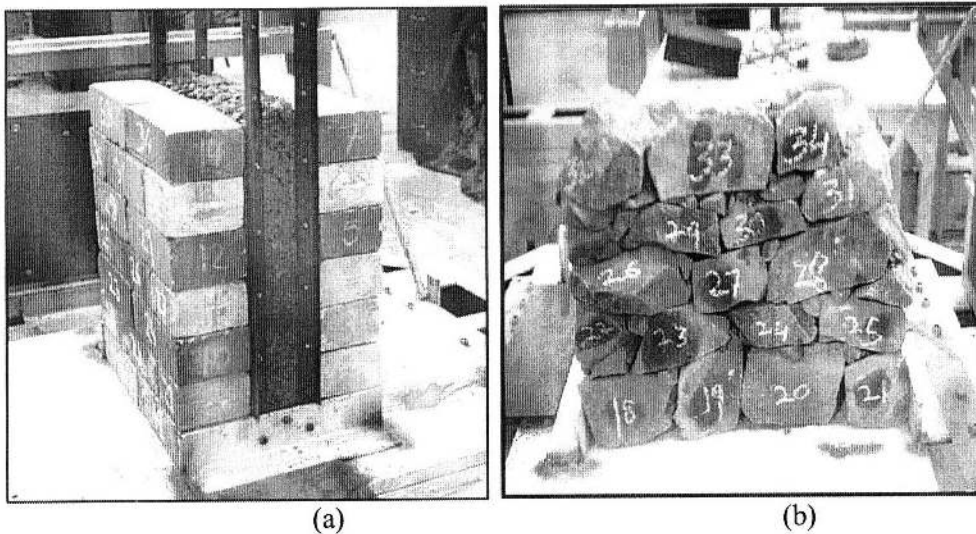


Figure 4-3. a) Brick wall with transparent infill boundary; b) typical stone wall.

4.4 Analytical Models: Brick Walls

UDEC was used to model the brick and stone walls with granular infill. This software allows taking a solid block and cutting it into multiple sub-blocks until the desired geometric characteristics are replicated. The material properties of the masonry units and gravel used in the construction of the physical specimens were mostly used in the analytical models with little correction necessary. To ensure that the angle of repose of the modeled granular material was similar to the actual one, a series of analyses were run by “pouring” the modeled granular material onto a surface (Figure 4-4a). Then the angle of repose was measured directly from the resulting graphical output of the analysis. The UDEC command “voronoi,” which randomly generates a series of cracks with an average pre-defined length (Figure 4-4b), was initially used to model the granular infill. However, it was observed that, depending on the degree to which the slopes of the cracks were aligned, the behavior or resulting model could vary significantly. Therefore, to obtain a homogeneous infill with fixed properties, the command “tunnel” was used to generate a granular infill made up of a large number of circular cracks (Figure 4-4).

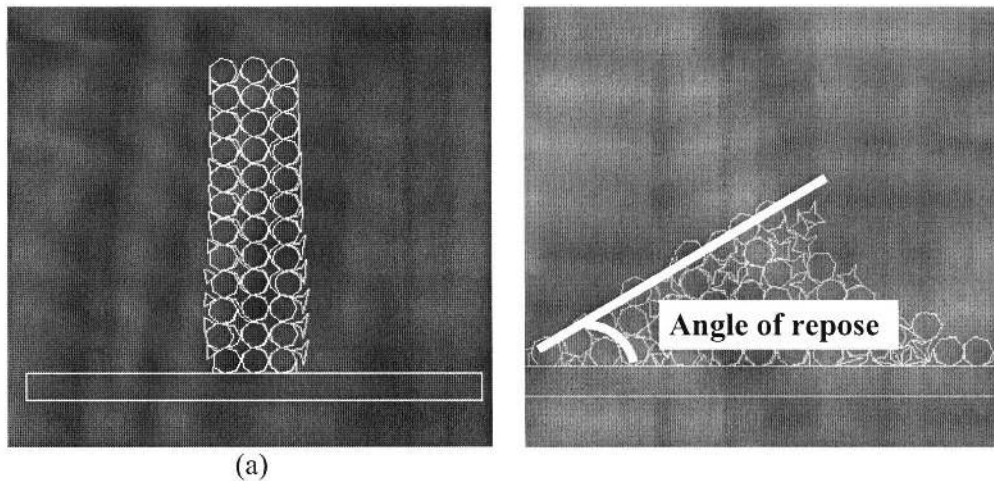


Figure 4-4. Gravel modeled with circular cracks: (a) before crumbling; (b) after crumbling, showing the angle of repose.

The static test series included changes in the wall height and infill width, as well as changes in infill friction angle. In the dynamic tests the wall height and infill friction angles were changed. In addition, the importance of the loading frequency and maximum acceleration were investigated. A sample of the scripts for the static and dynamic UDEC models can be found in Annex 2.

4.5 Analytical Models: Stone Wall Delamination

As mentioned in Chapter 1, wall delamination is a commonly observed failure mechanism of unreinforced stone masonry under seismic loading. Models illustrating this failure mechanism are shown in Figure 4-5.

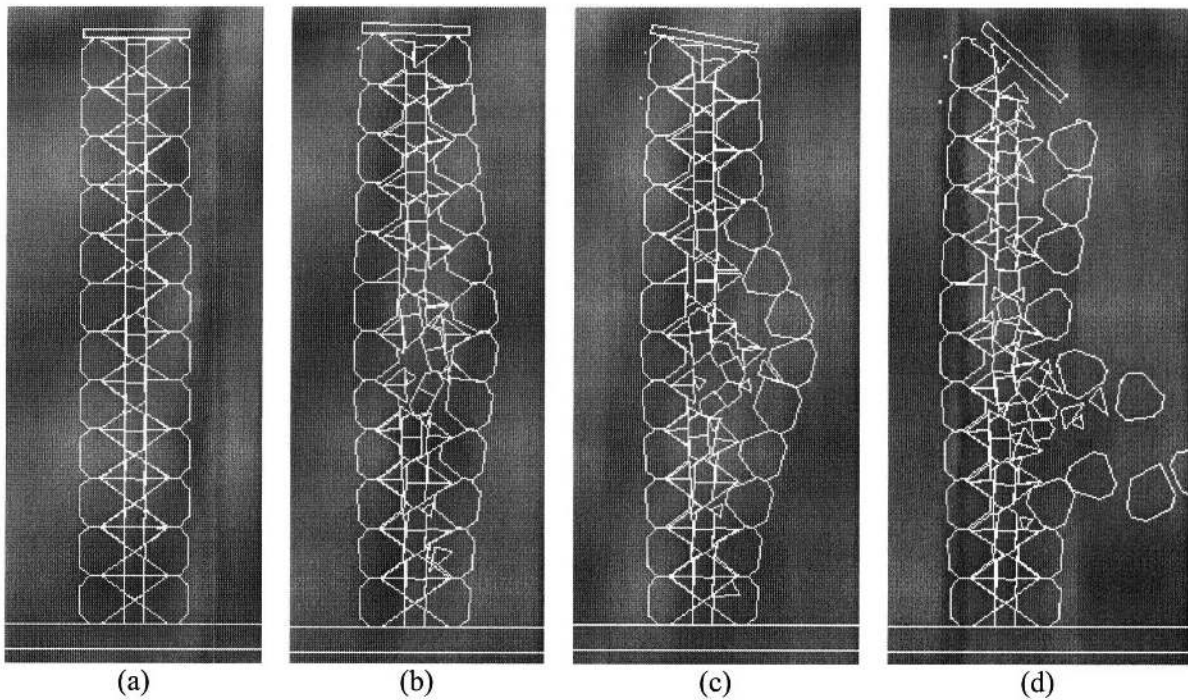


Figure 4-5. Wall delamination process.

The analytical models used to investigate the behavior of such walls consisted in two parallel wythes of stones with granular material as infill (Figure 4-6a). The material properties and dimensions of all the models analyzed were kept constant. The only change made to the model was the insertion of two and four through-stones to investigate their effectiveness in preventing wall delamination (Figure 4-6b). The loading accelerations were increased until failure of the model.

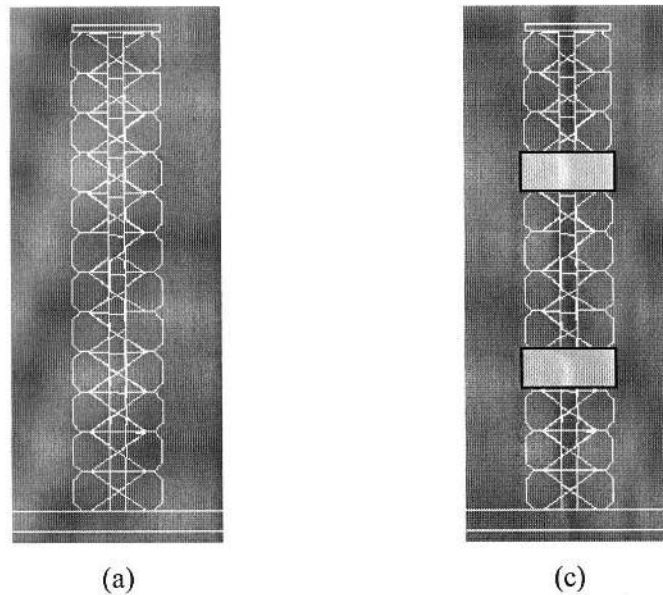


Figure 4-6.(a) Stone wall model; (b) model with through-stones.

4.6 Discussion

Take and Valsangkar (2001) have developed a model for retaining walls of narrow backfill width to calculate the pressures resulting from the granular fill acting on the interior of a retaining wall. This method was used for the preliminary analysis of the static behavior of the two-wythe brick walls with infill. This model shows a non-linear increase of the lateral pressures with depth due to the arching phenomenon, which predicted a static failure by overturning at a height of 60cm. The static failure of the physical models occurred, as predicted, by overturning. However, the failure height was consistently lower (average of 56cm) than predicted, mainly due to the irregularities in the bricks.

For the dynamic testing of the physical models, both horizontal and vertical vibrations were investigated at different frequencies and accelerations. Finally, the analytical models were used to investigate a large number of model variations, including wall height and width, and infill properties, for the static case. In the dynamic tests, the model height, the infill properties, and the loading frequency and accelerations were varied.

Finally, the problem of wall delamination of unreinforced stone walls and the commonly used through stone solution to this failure mechanism were modeled and investigated.

Chapter 5

5. Results

5.1 Static Tests: Brick Walls

Results from the eleven static tests indicate that the static infill pressure on the two wythes is significant enough to contribute to the damage of a wall. Overturning was the common failure mechanism and the size of granular infill was the main factor that influenced the failure height of the wall.

5.1.1 Influence of Granular Infill Friction Angle

The infill column height (i.e. wall height) needed for overturning failure increased with the increasing infill material friction angle (ϕ), which is consistent with the fact that larger friction angles cause a smaller lateral pressure. Figure 5-1 correlates the material's friction angles and the average wall failure height. The failure heights vary from 48cm for $\phi=31^\circ$ to 58cm for $\phi=38^\circ$, which represents a 20% increase in failure height.

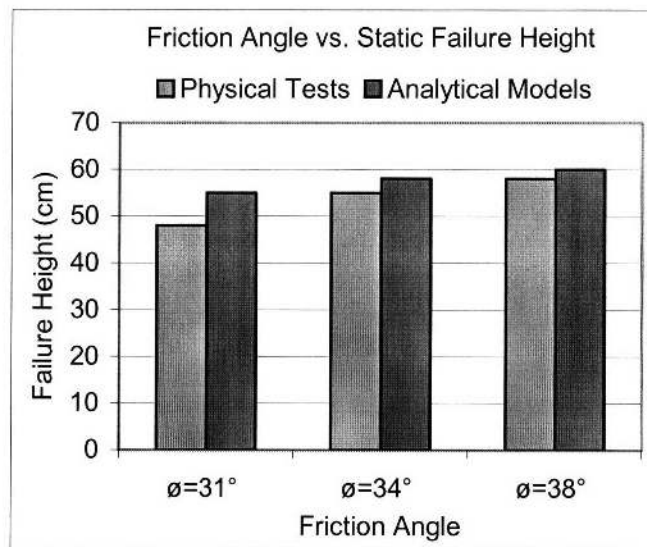


Figure 5-1. Effect of friction angle on failure height: increasing friction angle results in an increase of the wall failure height.

5.2 Dynamic Tests

5.2.1 Vertical Vibrations: Brick Walls

The dynamic failure mechanism of the brick walls at vertical accelerations below 0.4g was characterized, like in the static case, by the overturning of one of the wall wythes. However, the dynamic failures showed important differences from the static failure, most importantly that the failure onset occurred at 20% lower heights than in the static case. The full dynamic failure (without refilling the core material) occurred at wall heights 10 to 15% lower than the static failure, depending on the magnitude of the induced maximum vertical acceleration. In addition, the walls' failure process occurred gradually, unlike the sudden static failure.

A comparison plot of the wall heights needed for static and dynamic wythe overturning given the three different friction angles is shown in Figure 5-2, which shows that the dynamic failure height increases with increasing friction angle and that it is reduced by 20% (failure onset) from the static failure height. The consistent reduction in the wall failure height for the dynamic tests results from the increased lateral pressure caused by the shear fluidization and densification of the infill material undergoing vibration. When excited dynamically, the lateral pressure exerted by granular soils on the two wythes can be twice as high as the static pressure (Ni 1997). In addition, the lateral pressure exerted by the infill will increase further as a result of the removal of the arching effect, typical of granular soils in static conditions (Schulze 2005).

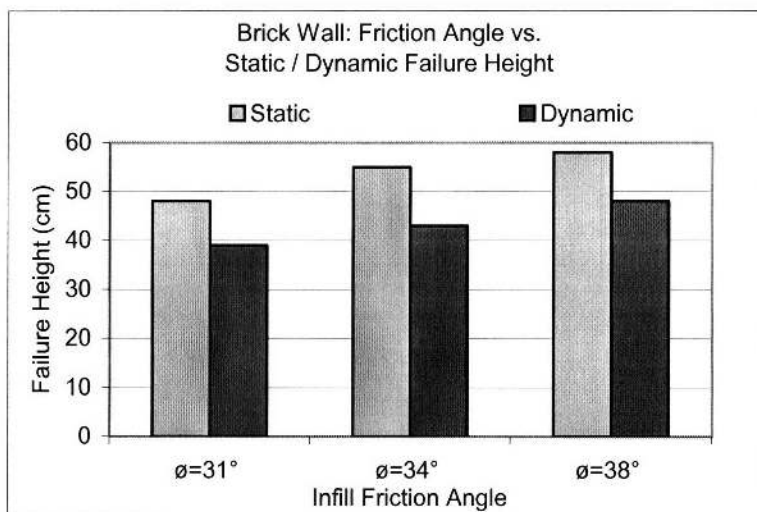


Figure 5-2. Friction angle versus static and dynamic failure heights for brick walls: increasing friction angle results in an increase of the wall failure height.

In some cases, the wall did not fully collapse after the onset of failure because the outward thrust was reduced due to the significant infill height reduction (Figure 5-4 and b). This height reduction was a result of the densification of the infill and the outward motion of the wall. In addition to the dominant overturning failure, it was observed that for the cases where the wall had vertical joints, the walls had a tendency to buckle outwards. This shows the importance of laying the masonry in a well-staggered manner and avoiding continuous vertical joints at the wall corners.

This series of dynamic tests reveals the two following trends. First, that the dynamic failure mechanism is characterized by overturning of one of the wythes and second, that the dynamic failure height is reduced by about 20% from the static failure height. In addition, as shown in Figure 5-3, the magnitude of the vertical acceleration has a significant role in the failure of the wall, reducing both the time to failure and the failure height of the walls.

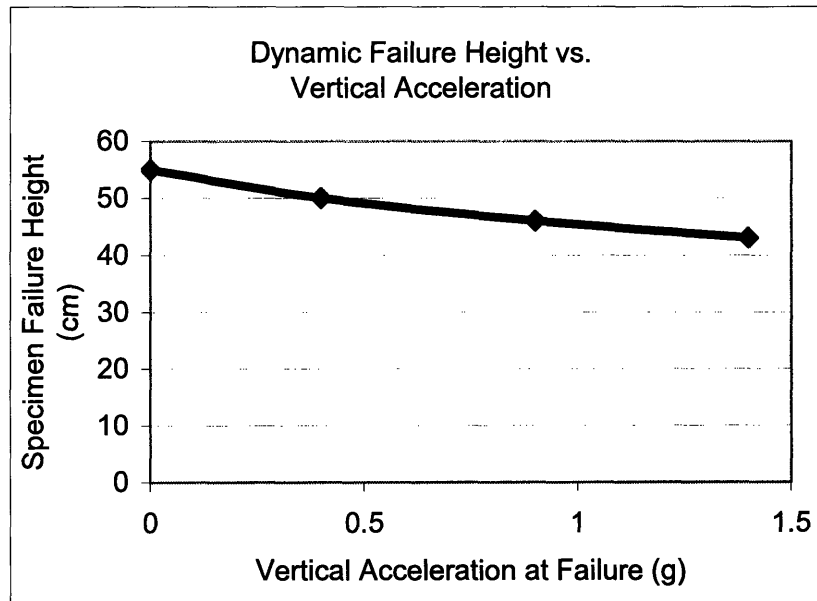


Figure 5-3. Frequencies and accelerations needed to induce overturning failure in brick walls

5.2.2 Horizontal Vibrations: Brick Walls

The brick dimensions used to build the walls on the shake table were different from the ones used in the vertical vibration tests. Therefore, a series of five static tests were conducted to find the average static failure height of 67cm. Two different wall heights were tested dynamically and found to fail at 37cm and 45cm respectively, which represent a 44 percent and 33 percent reduction from the average static failure height of 67cm. The static safety factors¹ for the dynamically tested walls were 1.4 and 1.3 respectively. The failure mechanism observed during the dynamic tests consisted of three distinct stages: infill densification, shear fluidization causing significant wall deformation, and wall failure. Table 5-1 shows a summary of the frequencies and minimum accelerations needed for these three stages to occur.

Table 5-1. Frequencies and minimum accelerations needed for the three failure stages to occur.

Failure Mechanism	Frequency (Hz)	Min. Acceleration (g)
Infill Densification	7	0.17
Shear Fluidization	9-20	0.2
Major Wall Deformation	9-20	0.3

The failure mechanism was initiated at an approximate frequency of 7Hz and accelerations not larger than 0.17g. At these frequencies, the granular infill densified and the arching effect was lost, resulting in an increase of lateral pressure on the two wall wythes. This densification continued for a short period of time and then the infill stabilized (Figure 5-4a). Infill densification resulted in a reduction of infill height, which in turn reduced the overturning moment caused by the internal pressure, and a slight outwards motion of the wythes (failure onset). In the cases where the infill was replenished, the wall failed without having to increase either the vibration frequencies or the acceleration.

The second failure stage occurred at frequencies between 9-20Hz and accelerations not larger than 0.2g. In this range of frequencies the granular infill underwent both densification and shear fluidization (Figure 5-4b). The shear fluidization of the infill sharply increased the lateral pressure on the two leaves, pushing them farther away.

The third failure stage occurred when frequencies between 9-20Hz were applied and the maximum acceleration was increased to about 0.3g. Under these conditions, the wall failed in

¹ Static safety factor = (Resisting Moment / Overturning Moment)

spite of a significant reduction of the infill height (reduction of the moment caused by the internal pressure), which in some cases became less than half of its initial height. In addition, the wall also showed significant lateral deformation (Figure 5-4c).

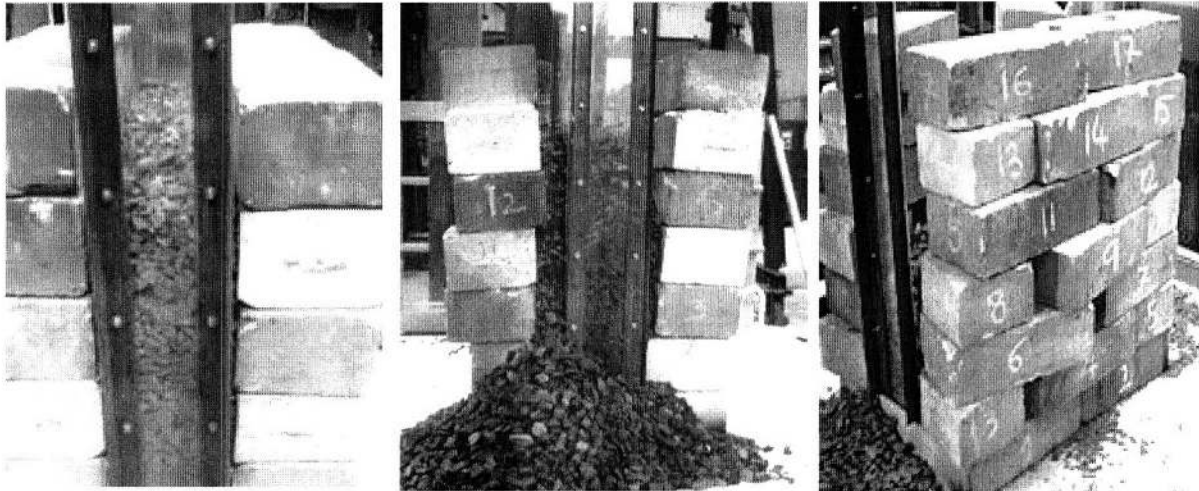


Figure 5-4. a) First stage: densification of the infill resulting in a reduction of 10% of infill height; b) Second stage: wall wythes are pushed apart due to increased internal pressure from shear fluidization of the infill; c) Third stage: walls either wholly deformed or collapsed.

These three failure stages can be correlated to the failure accelerations and frequencies of the individual walls shown in Figure 5-5. No failure occurred below 7Hz or 0.14g. The dynamic tests conducted under horizontal vibrations show that at vibration frequencies exceeding 10Hz and accelerations of 0.17g, the failure height is reduced by at least 35% from the static failure height. Furthermore, as Figure 5-5 indicates, the acceleration needed to cause failure increases with the vibration frequency.

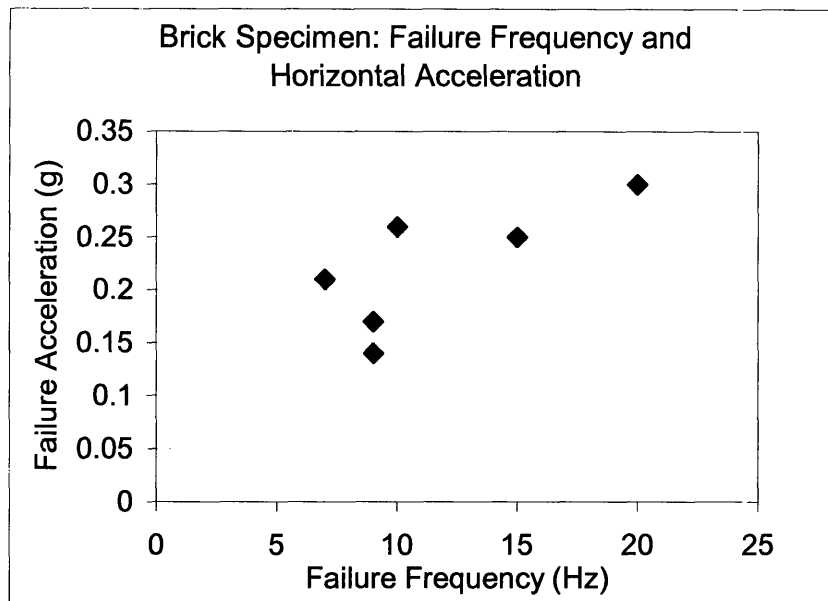


Figure 5-5. Frequencies and accelerations needed to cause full failure of the brick walls.

5.2.3 Horizontal Vibrations: Stone Walls

The results of the four dynamic tests show that the failure of the stone walls is dependent on vibration frequency, acceleration, and vibration time. In Table 5-2, a typical variable frequency testing procedure for stone wall #2 is shown. The first dynamic failure occurs at a vibration frequency of 11Hz and an acceleration of 0.17g and the final failure occurs at 15Hz and 0.28g. The damage of the wall progressed with time.

Table 5-2. Testing procedure for variable frequencies and maximum accelerations. Each sequence was held for two minutes (2nd stone wall).

Frequency Hz	Acceleration g	Comments
7	0.11	Stable
9	0.12	Stone dislocations
11	0.17	1st failure
13	0.12	Gravel flow
13	0.19	Gravel flow
15	0.28	2nd failure
17	0.29	Moving stones
19	0.38	Moving stones

The test results (Figure 5-6) indicate that a minimum horizontal vibration frequency of 11Hz and horizontal acceleration of 0.18g was needed to cause dislocation of the stones. That one wall

failed at the same frequency, but at the much higher acceleration of 0.36g, can be attributed to the difference in construction quality. To test the walls' response at high vibration frequencies, two walls were tested to failure at a constant frequency of 20Hz. The walls failed at 0.25g and 0.5g. As in the case of the brick walls, the experimental evidence shows that the acceleration causing failure increases with increasing frequency.

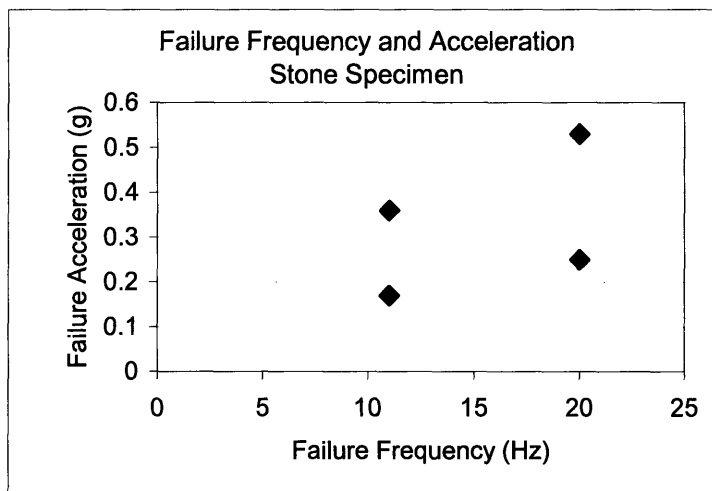


Figure 5-6. Failure frequencies and accelerations for stone walls.

Finally, it was observed that the vibration time proved to significantly influence the failure when the minimum failure frequencies and acceleration of 11Hz and 0.18g were exceeded. It was observed that the movement of the walls progressed with time, even when the frequency and acceleration were constant.

5.3 Analytical Model

5.3.1 Static Conditions

UDEC was used to simulate the static failure of the brick walls. The block and infill friction angles used in the model were the same as those used in the preliminary calculations. The coarse gravel-sized material (with $\phi=38^\circ$) was used as the basic infill for the model as seen in Figure 5-7a.

The failure mechanism obtained using the analytical model was almost identical to the failure mechanism of the physical walls, with a failure onset quickly followed by the overturning of the

wythes (Figure 5-7b and c). The failure height of the UDEC model was consistently higher than the failure height of the physical models. This height difference can be explained by the fact that the bricks used in the experiments were not perfectly rectangular, allowing for some initial out-of-plane movement of the wall wythes and reducing the overall stability of the wall.

It must be kept in mind that the failure height of the analytical model, as it was the case in the physical wall specimens, represents the height of the wythes and the initial granular infill height. The actual infill height will be significantly reduced, up to 50% from the initial height, due to spreading and overturning of the wythes. If the infill height were to be kept constant (by refilling the core space during the test) the failure heights would be lower and the difference between the static and dynamic failure height would be much larger. To overcome this difficulty, the initial outwards movement of the wythes, or failure onset, could be used as a reference to identify the failure of the model.

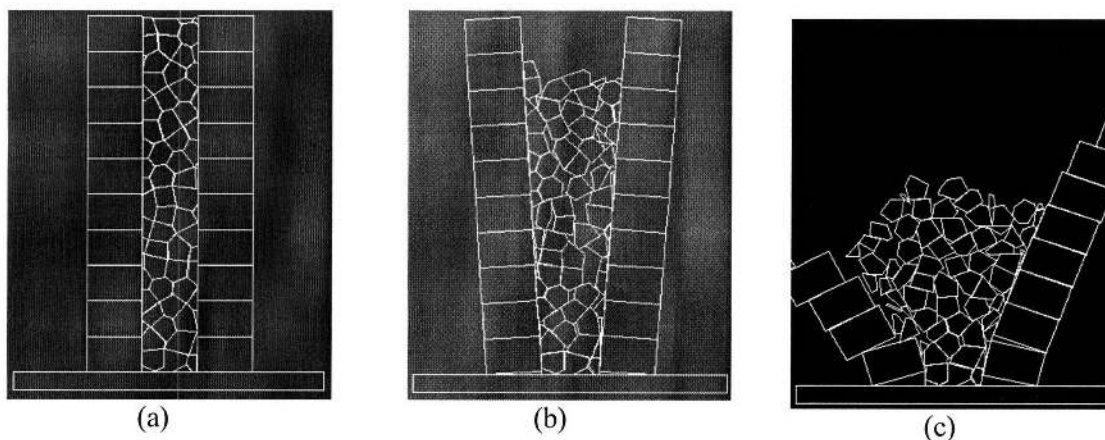


Figure 5-7. The UDEC static model with coarse gravel-sized infill material. a) Initial state of the model just after applying the gravitational force to the model; b) Failure onset after two seconds; c) Failed state after four seconds.

5.3.1.1 Variations in Infill Properties / Friction Angle

An analytical model with a brick and infill width of 15cm and varying height was used to investigate how the friction angle of the granular infill influences the lateral pressure exerted by the infill on the interior of the wythes. To ensure full consistency of the different models, the infill material was modeled as circular units of constant diameter instead of the previously used

randomly generated core material (Figure 5-8a). The friction angle was set to a value and models of different height were used to identify the height at which the model was about to fail for a given friction angle. Then the friction angle was increased and the impending failure height was found again.

The change in impending failure height for different friction angles is shown in Figure 5-8a. Between 55 and 85cm, the model showed a slow increase in the friction angle needed to keep the model stable when the wall height was increased. Then, between 85 and 115 the friction angle had to be increase much faster with increasing model heights. Beyond a height of 115cm, the model failed independently of the friction angle of the infill.

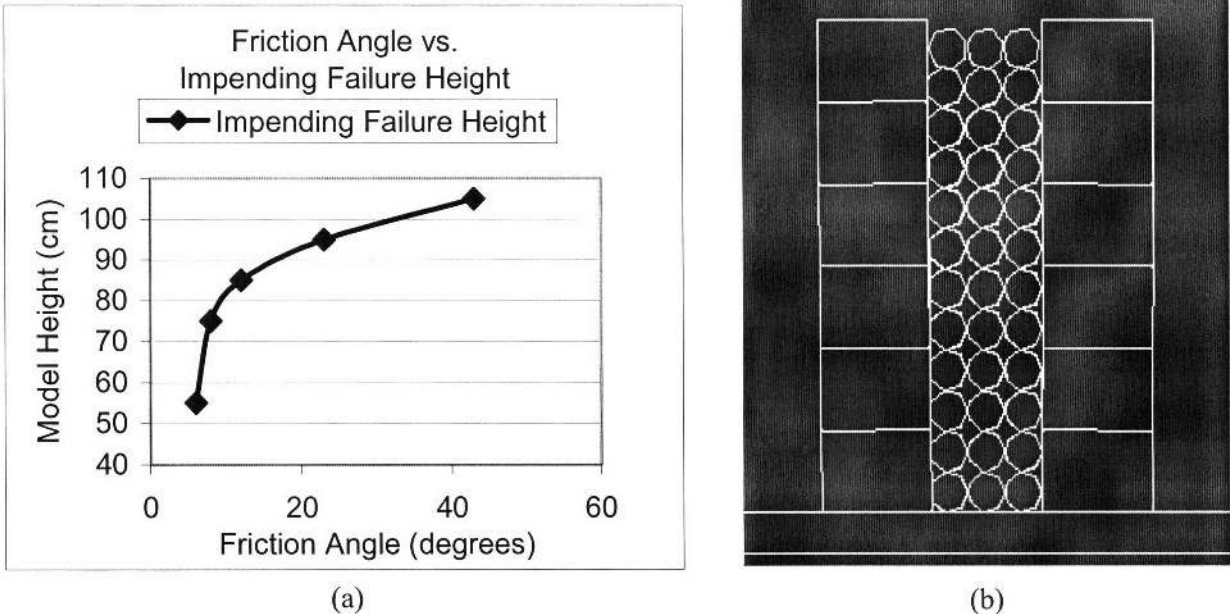


Figure 5-8. a) Plot of the impending failure height of the model given different friction angles of the infill material; b) Analytical model used with circular infill.

5.3.1.2 Variations in Wall Width

To investigate the effect of increasing the wall’s core width (Figure 5-10), a model with a constant height of 90cm was used. Then the width was increased and multiple analyses were run using different friction angles for the core material until the largest that would cause failure of the model was identified.

The plot in Figure 5-9 shows how a slow increase in the granular infill friction angle is needed to keep the model stable for an increase in infill width between 5 and 25cm. However,

beyond a width of 25cm, the friction angle has to be increased much faster with an increasing infill width. Furthermore, at infill width larger than 35cm the model failed irrespective of the infill's friction angle.

The failure mechanisms observed between infill widths 5-25cm consisted in initial outwards sliding of the block units, followed by the overturning of one or both wythes. The sliding became increasingly significant with an increasing infill width. The model with an infill width of 30cm failed by outward sliding of the two wythes (Figure 5-11).

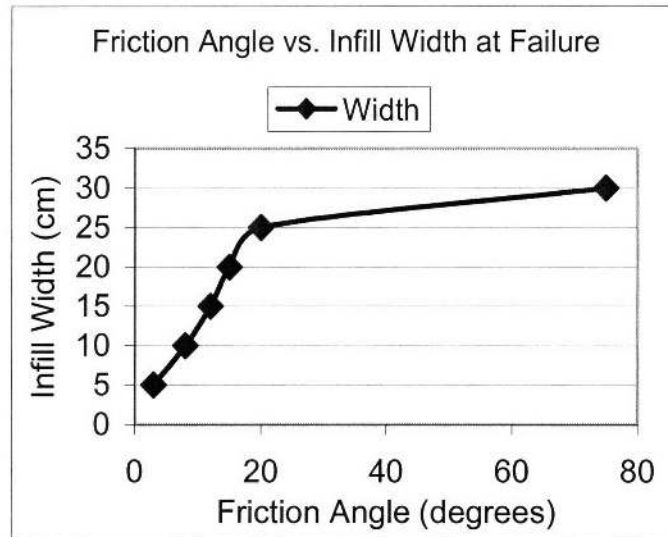


Figure 5-9. Plot of the infill material's friction angle needed to allow for a given infill width to be stable. A 90cm high model was used in all analyses.

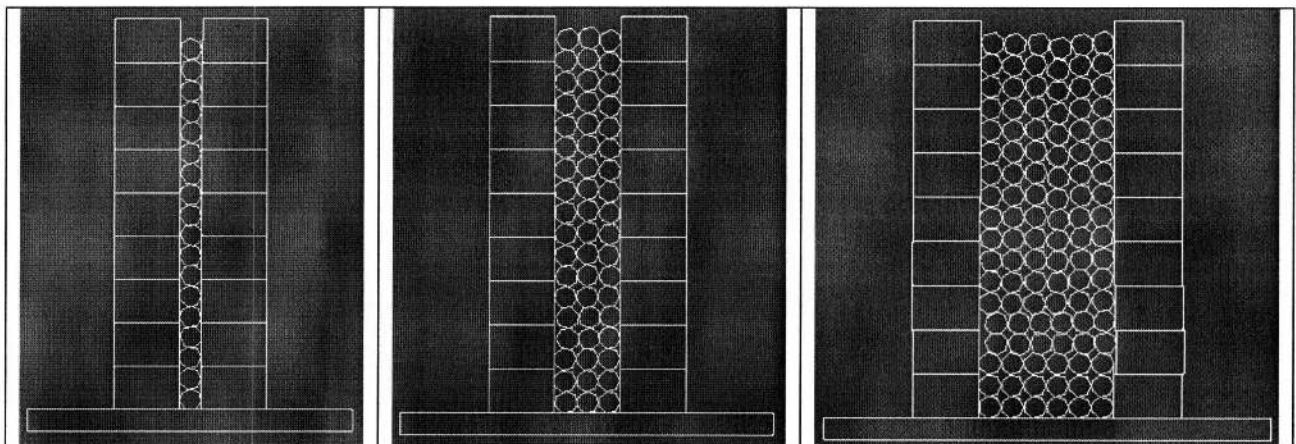


Figure 5-10. Models with constant height and varying infill width.

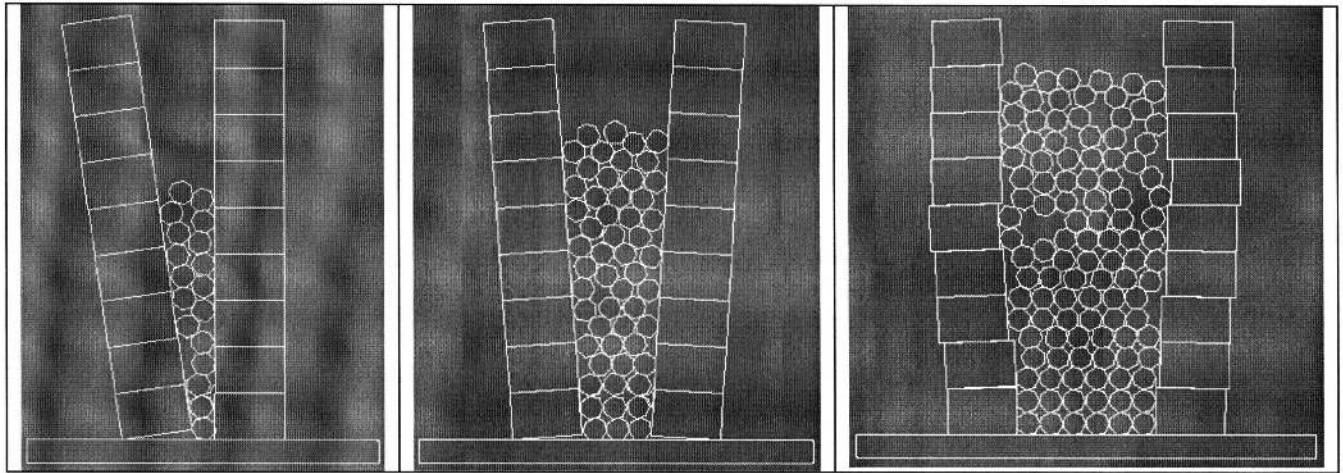


Figure 5-11. Failure modes for models of same height and different width.

5.3.2 Dynamic Conditions

5.3.2.1 Variations in Wall Height and Maximum Horizontal Acceleration

To investigate correlation between the wall height and the horizontal acceleration needed to cause failure, the friction angle of the infill and the bricks of the different models were kept constant ($\mu=35^\circ$ and 45° , respectively), while the height of the model was changed. From the loading side, a horizontal vibration was applied at a constant frequency of 20Hz, while the loading acceleration was increased to failure. It can be observed from Figure 5-12 that the acceleration needed to cause failure of the model is inversely proportional to the model height. The model failed statically at a height of 100cm and an acceleration of 1.4g was needed to cause its failure when the height was reduced to 60cm.

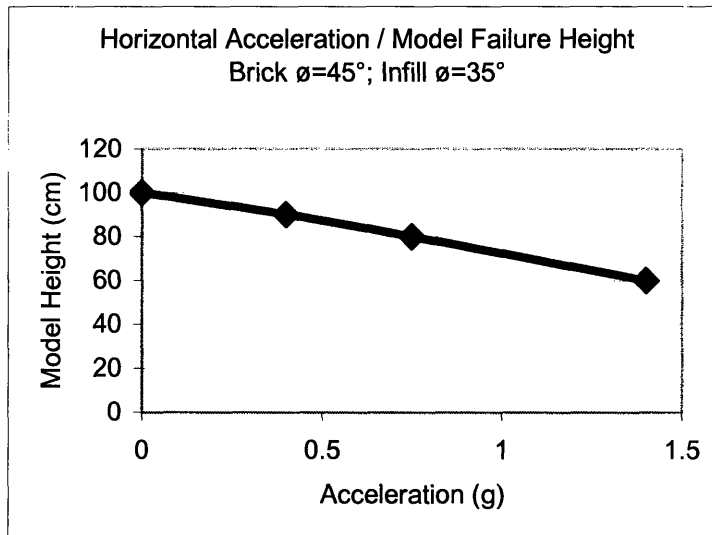


Figure 5-12. Horizontal acceleration needed to cause the failure with decreasing model heights.

5.3.2.2 Variations in Wall Height and Maximum Vertical Acceleration

As in the previous section, to study the correlation between the wall height and the vertical acceleration needed to cause failure the friction angle of the infill and the bricks of the different models were kept constant ($\phi=35^\circ$ and 45° , respectively), while the model height and the loading acceleration were changed. The vertical vibration was applied at a constant frequency of 20Hz, while the loading acceleration was increased to failure. It can be observed from Figure 5-13 that, as it was the case for horizontal acceleration, the vertical acceleration needed to cause failure of the model decreases with increasing model height. However, it is interesting to note that the vertical accelerations at failure are consistently lower than the horizontal accelerations needed to cause the failure of the model. This shows the importance of taking into account the vertical component of the seismic vibrations during the structural design process.

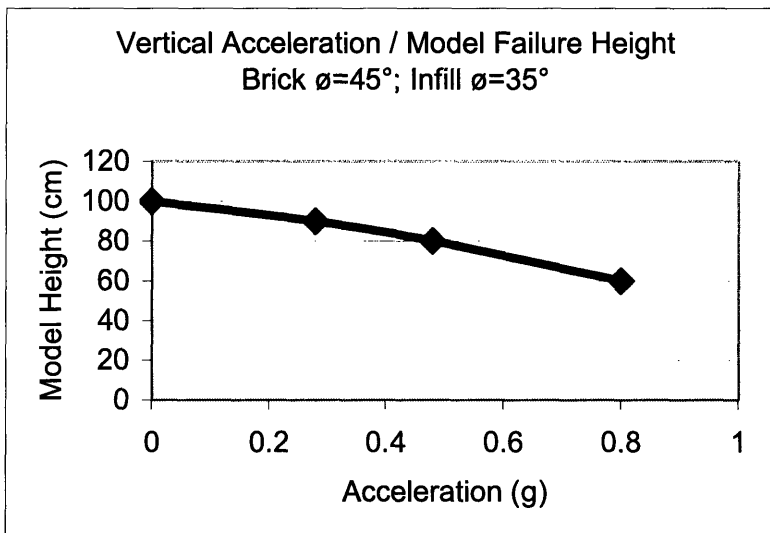


Figure 5-13. Vertical acceleration needed to cause the failure with decreasing model heights.

One example representative of the difference in behavior of the models subjected to individual 20Hz vertical or horizontal vibrations is the case of the 60cm high wall model seen in Figure 5-15a and b. This model failed at a maximum acceleration of 0.5g when vibrated vertically, while it did not fail even at accelerations over 1.7g (much higher than encounter in real life) when vibrated horizontally. Moreover, the failure mode of the model subjected to vertical vibrations was mainly through sliding of the different blocks.

5.3.2.3 Simultaneous Vertical and Horizontal Vibrations

When simultaneous horizontal and vertical vibrations were induced, it was observed that the sliding of the blocks and subsequent failure occurred at smaller loading accelerations. Examples of this failure behavior were the 60cm high models shown in Figure 5-15 that were both vibrated at 20Hz and with an acceleration of 0.8g. The model in Figure 5-15a was excited in both vertical and horizontal directions, while the model in Figure 5-15b was only vibrated in the horizontal direction. The model vibrated in both directions fully failed, while the other model remained stable after an initial overturning motion.

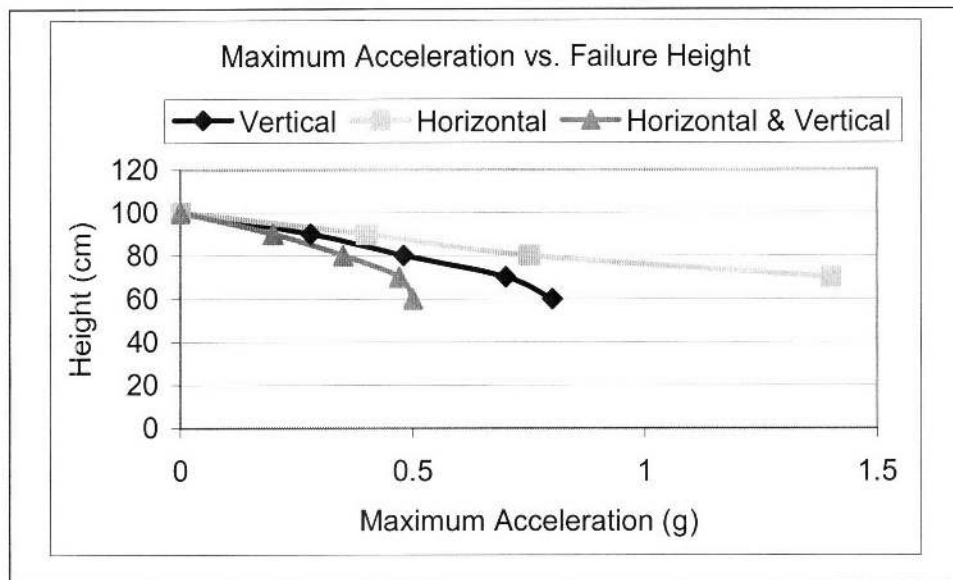


Figure 5-14. Plot showing the maximum acceleration needed to cause failure of a specimen of a given height.

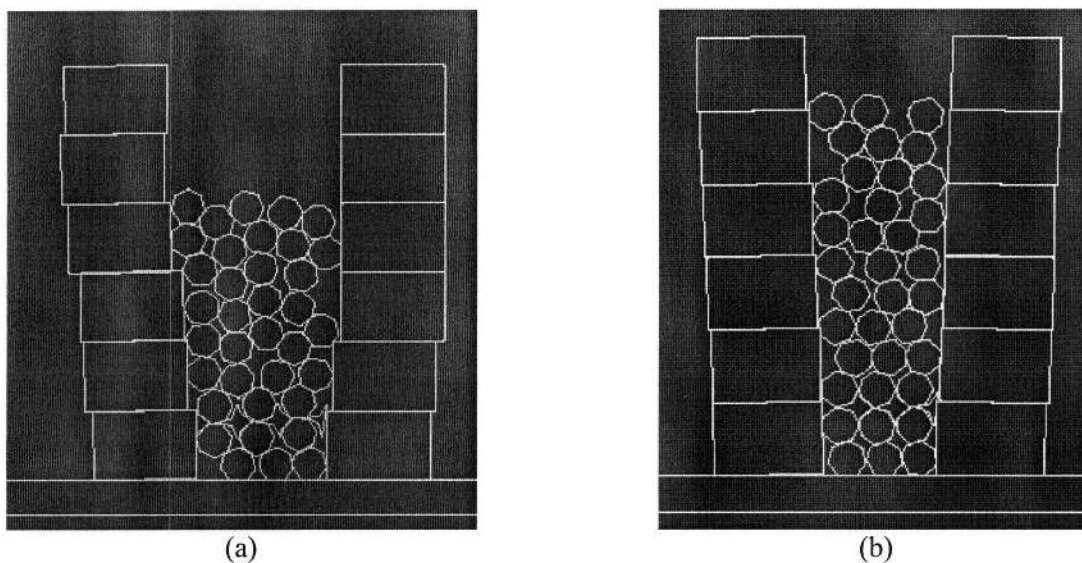


Figure 5-15. a) Model failing through sliding of the bricks; b) Model after initial rotation of the wythes.

5.3.2.4 Wall Delamination and Through-Stones

The model with no through-stones (Figure 5-16a) failed by delamination at an acceleration of 0.19g, while neither of the other two models, which had two and four through-stones inserted (Figure 5-16b and c), failed at this acceleration. The models that had two and four through-stones inserted failed at accelerations of 0.32g and 0.45g, respectively.

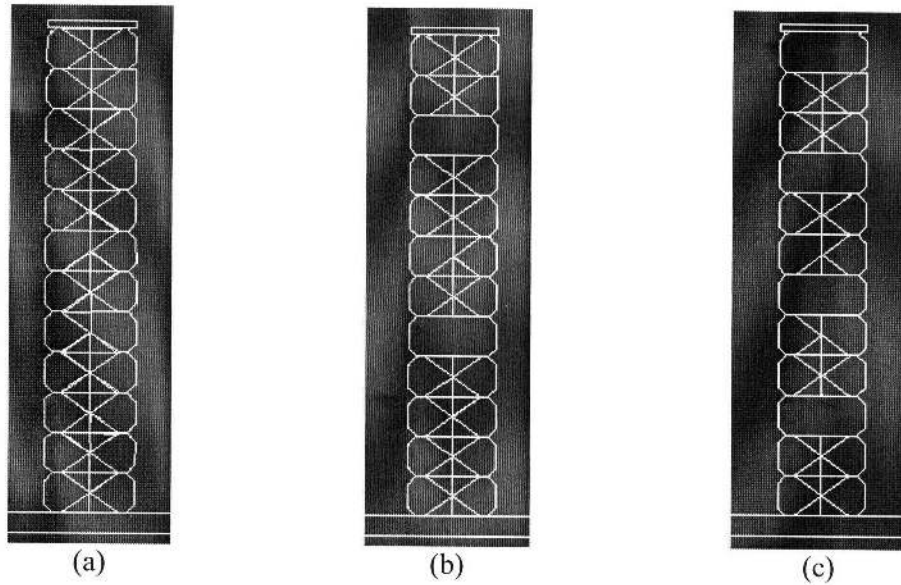


Figure 5-16. (a) Model of two-wythe stone walls without through-stones; (b) Model with two through-stones; (c) Model with four through-stones.

As can be observed in Figure 5-17a, the failure of the model with no through-stones did not only fail at a significantly lower loading acceleration, but it also failed in a catastrophic manner, dissipating only limited energy during the failure process. The models with through-stones (Figure 5-17b and c) deformed significantly before fully failing. This shows that the use of through-stones will provide much needed ductility in seismic events to unreinforced stone masonry structures.

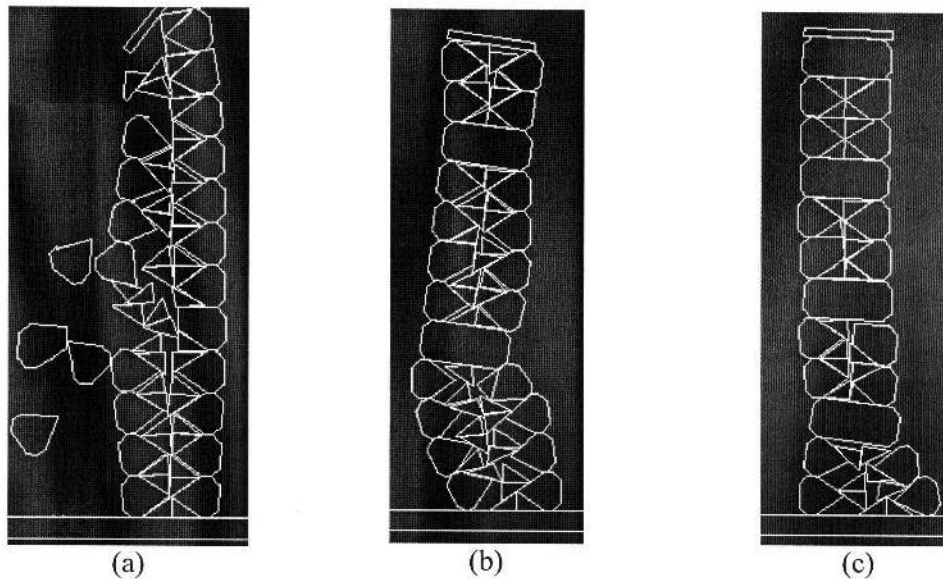


Figure 5-17. (a) Failure at 0.19g; (b) Failure at 0.32g; (c) Failure at 0.45g.

Figure 5-18 shows how the acceleration needed to cause the failure of the model increases with an increasing number of through-stones. These results clearly indicate that the use of through-stones in the construction of unreinforced stone masonry walls can significantly improve their dynamic performance.

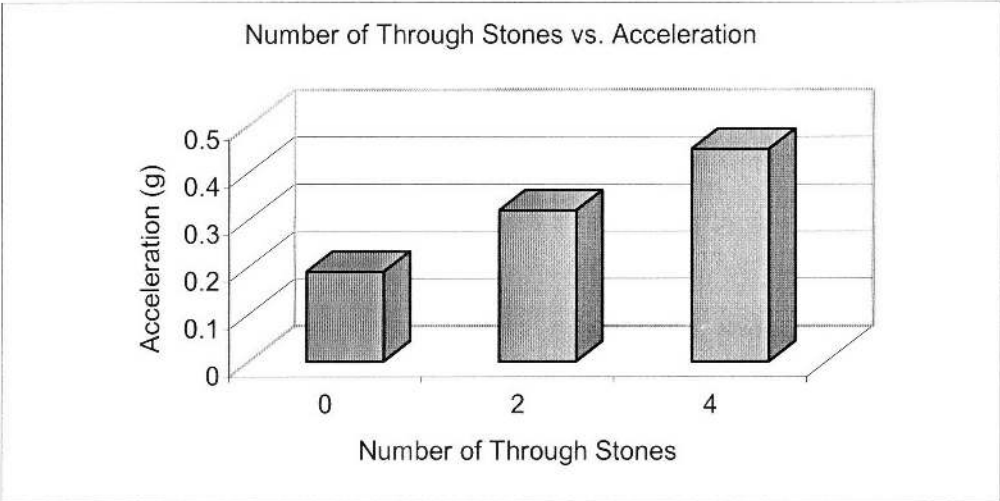


Figure 5-18. Plot of the acceleration needed to cause the failure of the models with different numbers of through-stones.

5.4 Discussion

The results obtained from the static tests of two-wythe brick masonry walls with granular infill clearly indicate that the outwards pressure of the infill can contribute to the overall failure of the wall. Moreover, the lateral pressure on the inner part of the wall coming from the infill will increase with decreasing friction angle of the material. The dynamic failure of the same brick walls, for both vertical and horizontal accelerations, occurs at heights at least 15% lower than the static failure. In addition, if the acceleration is increased, the wall failure height decreases and can be up to 35% lower than the static failure height.

The dynamic (horizontal vibrations) tests of the stone walls showed that a minimum frequency and acceleration of 11Hz and 0.18g, respectively, were needed to cause the dislocation of the wall. In addition, the fact that the specimens also failed at 20Hz and 0.25g shows that high frequency / low-energy vibrations can cause the failure of dry stone masonry.

The static tests of analytical models of the walls confirm that a reduction in friction angle of the infill will also result in a reduction of the failure height. The only difference between the physical and analytical tests being that the failure height of the model was increased by 5-10%. Additional results also showed that an increase in infill width results in an increase of the internal normal pressure on the wythes, and therefore, a reduction in failure height. This is probably due to a reduction of the significance of the arching effect and vertical shear force on the walls coming from the infill. For the case of dynamic loading, the analyses indicate that vertical vibrations are more detrimental than horizontal ones, and that it is the combination of vertical *and* horizontal vibrations that cause the models to fail at the lowest loading accelerations. In addition, the problem of wall delamination was investigated. The results clearly indicate that the introduction of through-stones will increase the stability and ductility of the wall.

Finally, these series of empirical and analytical tests show that high frequency / low energy seismic vibrations can be significant enough to cause failure of an unreinforced masonry structure.

Chapter 6

6. Low-Cost Remedial Actions

This chapter describes a series of low-cost, low-tech remedial actions that can make a significant difference in the seismic performance of both unreinforced brick and stone masonry. It is important to note that the objective of these construction improvements is only to provide those with no or very limited economic resources with the means of reducing the damage to their houses and the harm to their dwellers. However, these strengthening methods will *not* make the structures “earthquake-proof” because of the inherent structural limitations of unreinforced masonry under seismic loads. Construction improvements for new construction and retrofit methods for existing buildings will be considered.

6.1 New Construction

After recent catastrophic earthquakes it might be assumed that the construction practices in new structures would discard previous obviously inadequate construction practices. This, however, is not the case in developing countries, where most of the unreinforced, poorly built structures are located. The author has visited several regions—Izmir, Gujarat, Bam, Lijiang—in the aftermath of major earthquakes and has consistently observed that, in the cases where URM was still used, the construction practices neglect to integrate the basic improvements needed to build stronger structures. Some of these low-cost improvements are described in the next sections.

6.1.1 Through-Stones and Stone Shape

The introduction of through-stones is the most effective solution to the extremely common problem of wall delamination (Figure 6-2a and b). This solution has been proposed by Murthy (2003), among others, and is well known among the experts in URM. However, it seems that it has yet to reach the people who need to implement this technique. Besides preventing wall delamination, through-stones could also significantly slow down the wall disaggregation process resulting from shear fluidification.

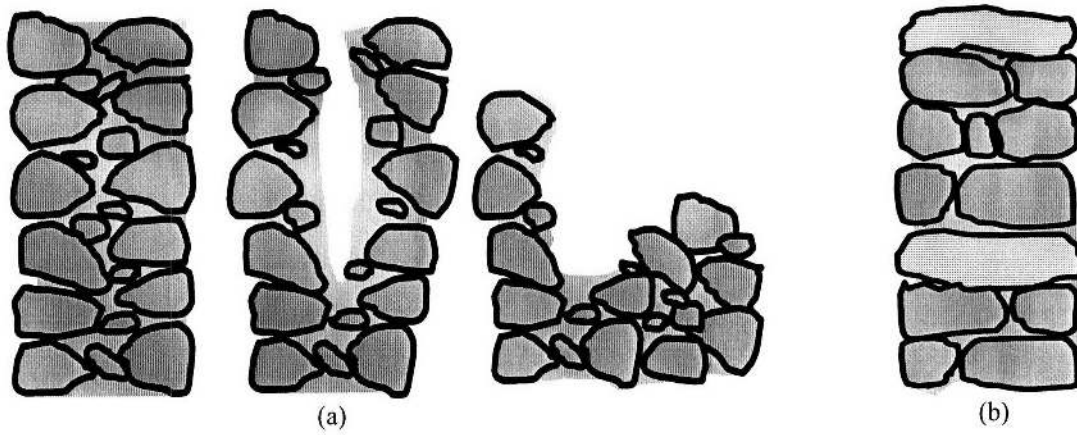


Figure 6-1. (a) Delamination of a dry stone wall with no through-stones; (b) through-stone solution.

As seen in Figure 6-2a, the introduction of through-stones in the wall has to be done at horizontal and vertical staggered intervals of minimum 50cm and 70cm, respectively. It is preferable that large, long stones be used to ensure proper connection of the two wall wythes. In the event that long enough stones are not available, a combination of four smaller stones can be used to achieve the same effect (Figure 6-2b).

The shape of the stones is one of the key issues in building a safe stone house. It is very important to use cubical and rectangular stones of similar size and to avoid oblong, rounded, and small stones. The stone shape and size are crucial in the corners, where it must be ensured that large rectangular stones are used and are laid alternating the long sides, as seen in Figure 6-2a.

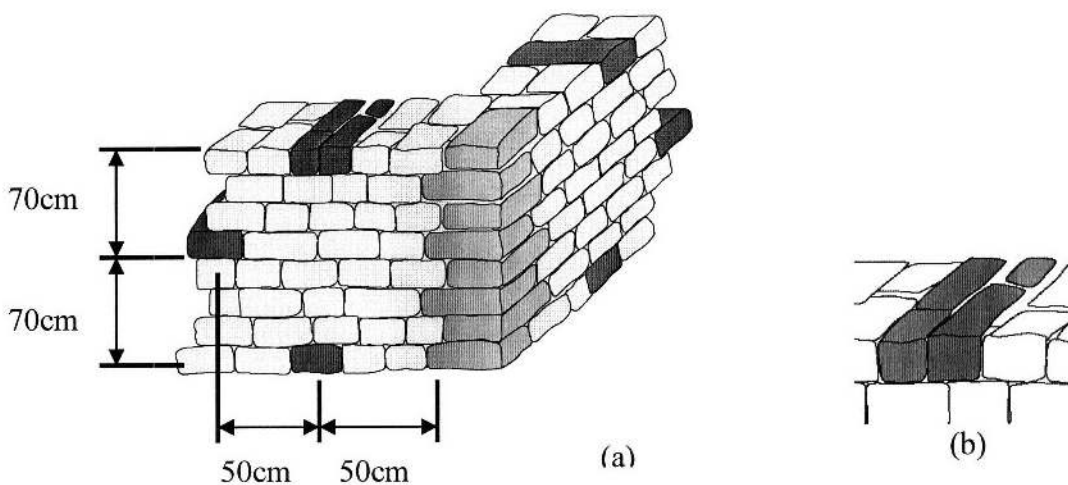


Figure 6-2. (a) Wall corner with through-stones and big, uniform corner stones; (b) through stone made with four units of smaller stones.

6.1.2 Distribution and Proportions of Openings

The overall stability of the structure can also be improved by following the appropriate opening proportions and distribution. Commonly accepted opening proportions can be found in Figure 6-3, which can vary depending on the quality of the construction and the size and shape of the stones used. By respecting these dimensions crack initiation and propagation in unreinforced stone houses will be significantly reduced.

The distribution of the openings around the house is also to be taken into account when deciding where to position them, because an inappropriate distribution could result in torsional forces on the structure. Therefore, it should be ensured that the overall center of stiffness of the house be kept close to its center of mass.

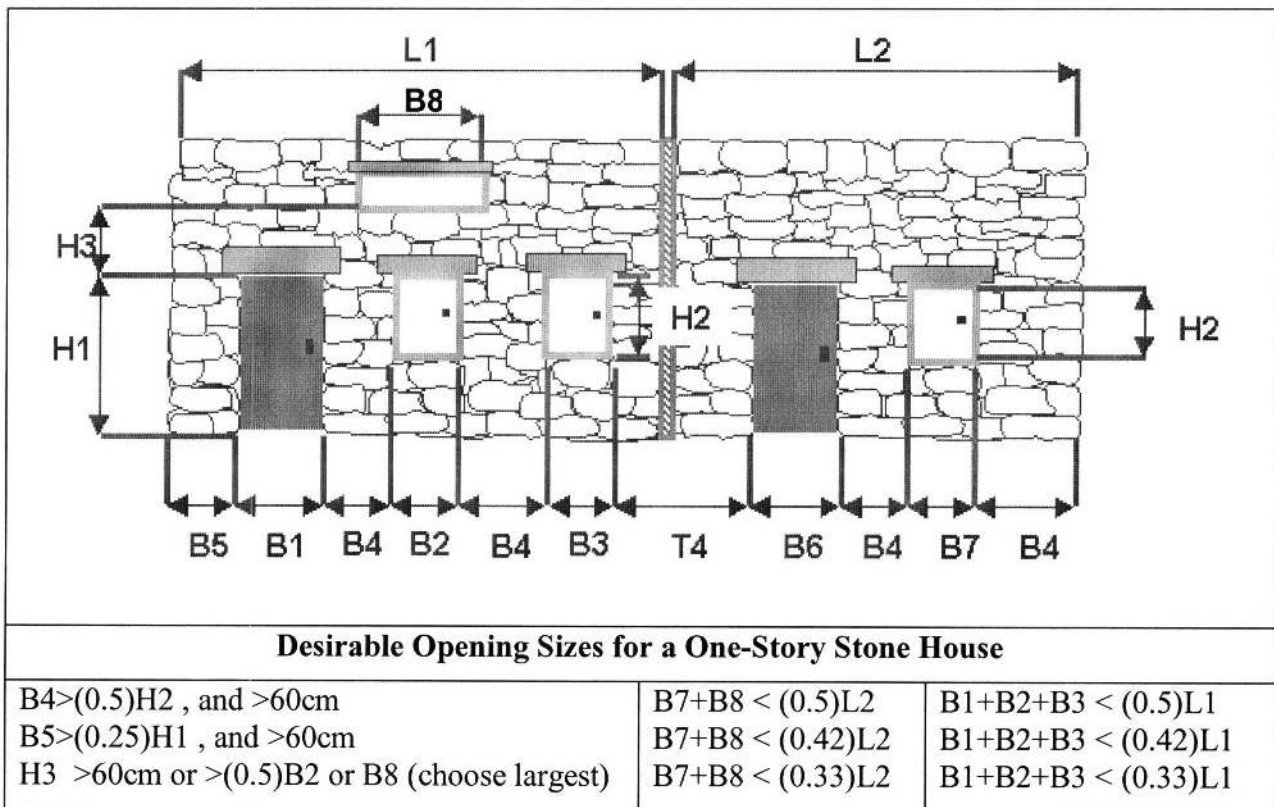


Figure 6-3. Recommended opening proportions for a one-story, unreinforced stone house (Source: Arya 2005).

6.1.3 “Hanchiku” Seismic Base Isolation

A method of building earthen foundations using alternated layers of loose sand and fat clay was introduced to Japan from China fifteen centuries ago (<http://www.aisf.or.jp/~jaanus/deta/>

[h/hanchiku.htm](http://hanchiku.htm)). This same method was then used as a base isolator for temples and other important structures. “Under the building to be protected, a cushion of fat clay with enclosed loose sand layers is placed and kept water-saturated. Base shaking by a strong earthquake leads to degradation of shear stiffness in the first cycle so that further shear waves cannot reach the building,” as seen in Figure 6-4 (Gudehus 2004).

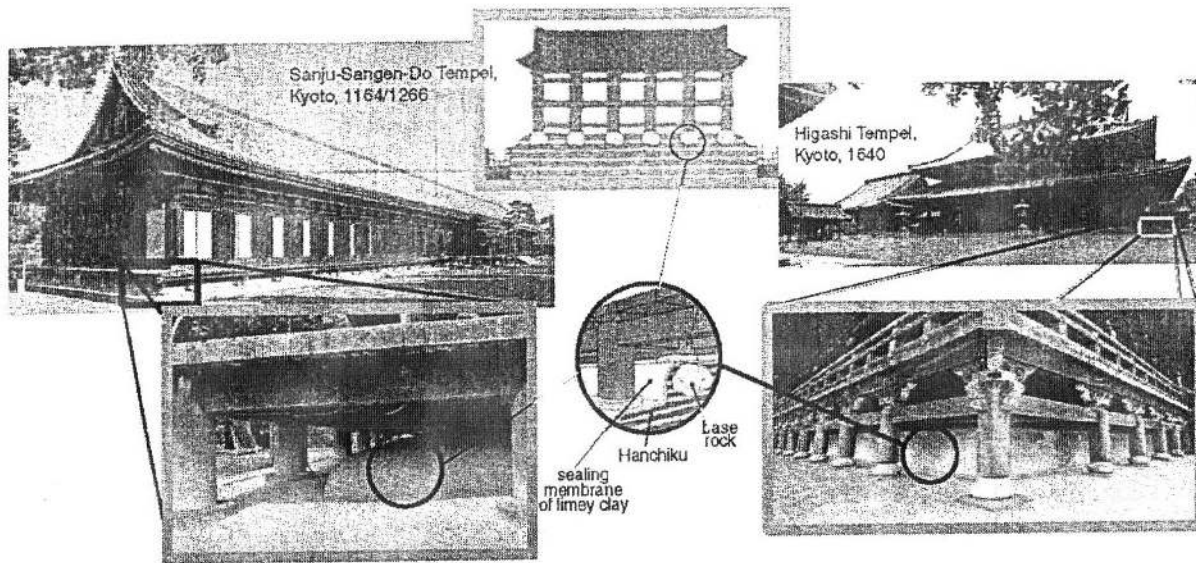


Figure 6-4. “Temples in Kyoto with Hanchiku seismic isolation. The inlets show confining seal of chalky clay and base rocks to keep settlements at acceptable limits.” (Source: Gudehus 2004)

The Hanchiku seismic isolation principle could be implemented in low-cost housing too. One way proposed by Gudehus (personal conversation) is to align a series of old tires at the foundation level and fill them with a layer of fat clay, a layer of loose sand, and again a layer of fat clay. This way the desired base isolation can be achieved without a major investment. The drawback of this system is that the saturation of the sand layer must be continuously maintained; otherwise, it will not perform adequately.

An additional low-cost base isolation system, still to be investigated, is the mixing of rubber pieces (from old tires, for example) with the stones that make up the foundations. By mixing rubber pieces, in a stone/rubber volume ratio to be determined, the high frequencies (above 10Hz) seismic vibrations could be significantly filtered out, and thereby preventing the damage caused by the previously described shear fluidization. This foundation system, however, will not isolate the structure from lower frequencies, which can be the source of major structural damage.

6.2 Retrofit

A structurally deficient house can be retrofitted by introducing a number of structural upgrades that will improve its performance during an earthquake. However, it is important to first assess the adequacy of the overall structural strength to ensure that it is worth upgrading. The seismic performance of a seriously deficient structure will only be marginally improved by retrofitting it because the improvements will ultimately not be engaged during a seismic event. Therefore, the owners should be informed of the risk and advised to demolish and rebuild it. Retrofit of a severely deficient house will only mislead its dwellers into believing that they will be safe in it in the event of an earthquake.

There is no one-for-all type of retrofit method. The choice of the retrofit system used will depend on the type of structural deficiency, the materials used in the structure, the availability and cost of construction materials, the available construction skills, and the cost that the homeowners are willing to pay for the improvement. Only simple, low-cost retrofit methods for unreinforced stone masonry houses are considered in the next section, including through-stones, cementitious mortar, partition of long rooms, and roof-wall connection systems. These retrofit methods are commonly found in the literature concerned with the retrofit of low cost housing, however, the two roof-wall connection systems presented here have yet to be tested empirically to assess their performance.

6.2.1 Through-Stones and Cementitious Mortar

The simplest and cheapest solution to prevent two major failure mechanisms in unreinforced stone masonry, wall delamination and crumbling, is to replace some of the stones that make up the individual wythes by through-stones. This will be achieved by carefully removing a stone (or more, if needed) at the same height on each side of the wall, which will leave an open cavity across the wall. The stones to be replaced should preferably be small. Then, a stone of a length at least equal to the wall width and with volume similar to the cavity is to be placed in the cavity and laid in a cementitious mortar. As mentioned earlier, the through-stones should be spaced at less than one meter horizontally and seventy centimeters vertically; in addition, the different horizontal rows should be staggered with respect to each other. In the event that large enough stones are not available, a concrete block or steel hook can be used instead. In this case, it is key to ensure that the cavity is fully grouted with cement mortar.

In a many low-cost stone houses, the stones were laid in mud mortar (Figure 6-5a), which will easily crumble when vibrated, leaving large voids around the stones (Figure 6-5b) and inducing wall crumbling. Ideally, the mud mortar should be removed as far as the available tools can reach into the wall, and then replaced by a cementitious mortar, to prevent further wall delamination and crumbling.

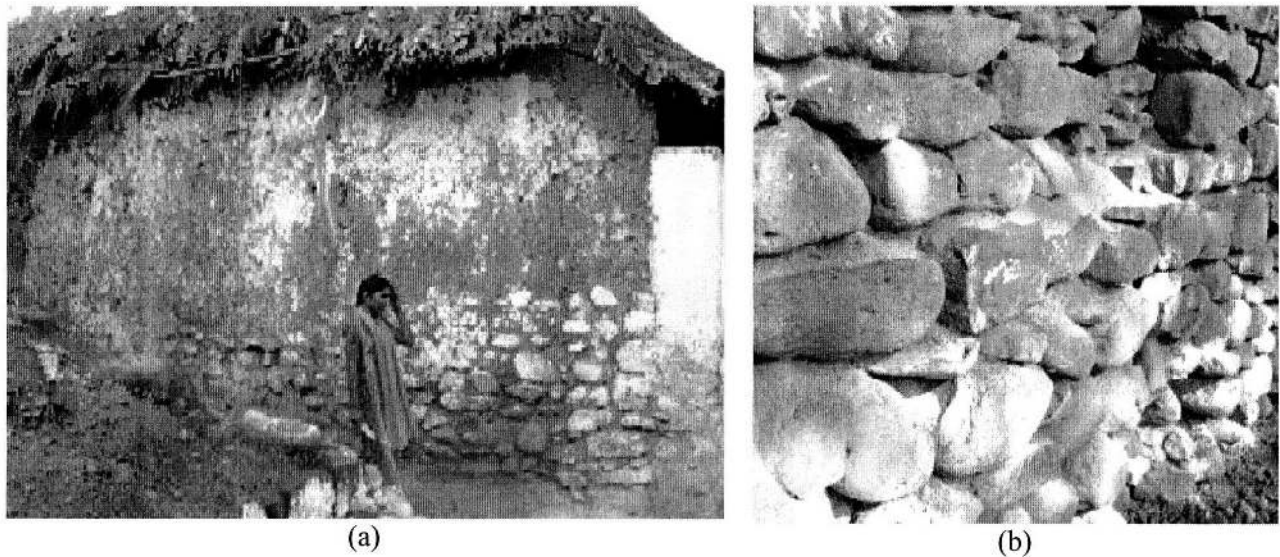


Figure 6-5. (a) Stone laid in thick mud mortar; (b) dry mud mortar falling out of the joints leaving voids around the stone units.

6.2.2 Room Partitions

The out-of-plane wall failure is a commonly occurring failure mechanism in URM. The individual walls of an unbound structure act independently of each other and, therefore, are very weak in resisting loads perpendicular to their planes. This is particularly true in the case of long continuous walls, as shown in Figure 6-6.

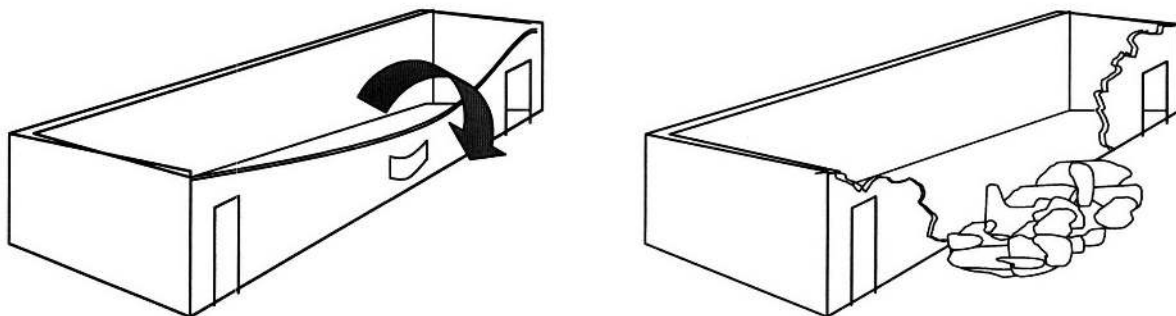


Figure 6-6. Out-of-plane failure of a long, continuous wall.

The ideal solution for such long continuous walls is to introduce partition walls to supply restraint. If there are no restrictions, the proportions of the partitions that should ideally be achieved are the ones shown in Figure 6-7, where $a/t < 40$.

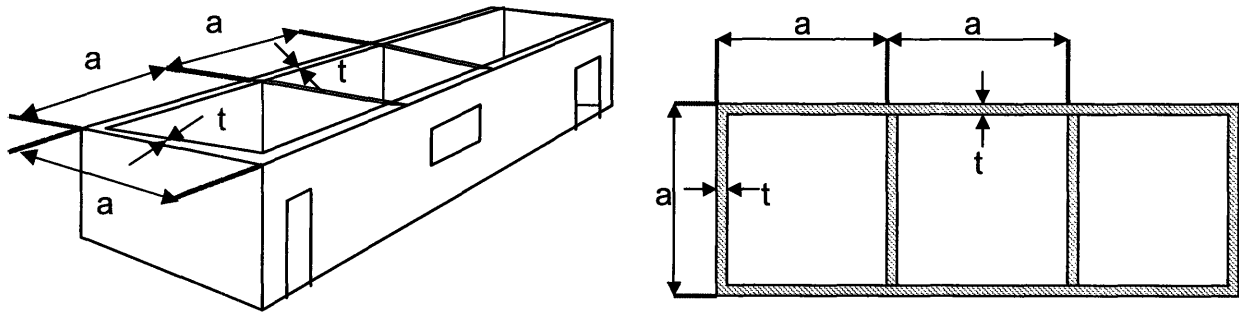


Figure 6-7. Introduction of cross-wall to improve the out-of-plane behavior.

Introducing cross-walls is often not possible, or is insufficient to prevent out-of-plane failure, particularly in the case of dry stone masonry. In such situations, it is necessary to introduce a retrofit system that, by structurally connecting them, will transform the individual actions of the four walls into a box action. This can be achieved by taking advantage of the roofing structural system, that more often than not consists of trusses or robust beams. The two retrofit systems proposed next were developed for the region of Kashmir, Pakistan, taking into account that the cost as well as the skills needed for the implementation should be kept to a minimum.

6.2.3 Roof-Wall Connection I

The first system proposed consists of a series of dowels (wood or steel) being inserted into the wall. Then, a wire is attached at one end of the dowel and run over the roofing structural member running along the top of the wall and then down the other side of the wall, tying it to the other end of the dowel (Figure 6-8). By interconnecting the walls through the roofing members a box effect can be achieved. An additional benefit of this retrofit system is that the effect of a ring beam can be obtained by post-stressing the top part of the wall with the wires. For this system to

perform adequately, the stiffness of the roof has to be large enough to allow for the load transfer. The roof stiffness should be improved if it is too small.

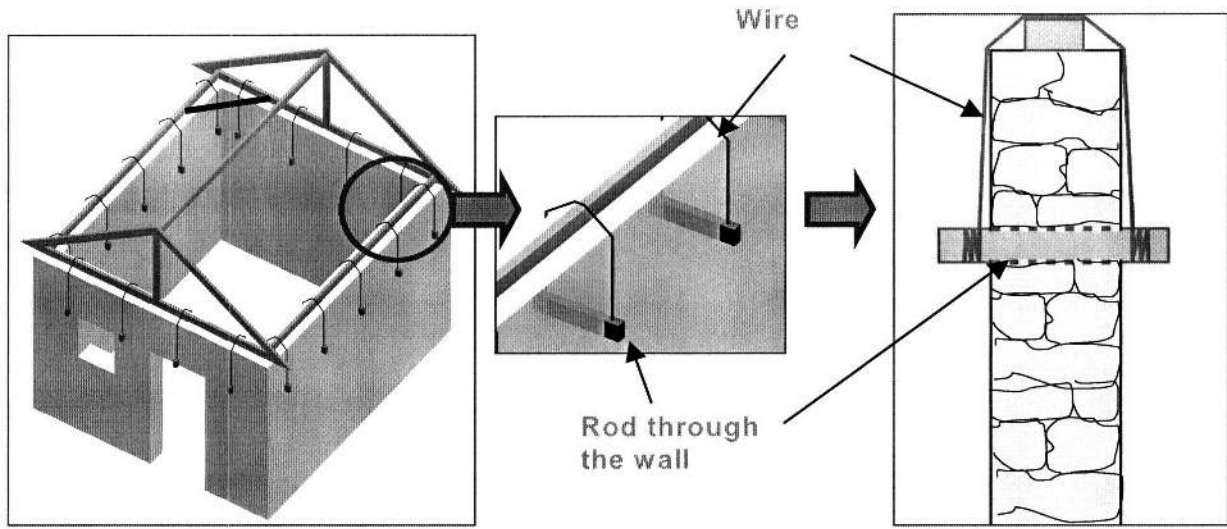


Figure 6-8. Roof-wall connection system using dowels and wires (Drawings by: Yanni Loukissas).

6.2.4 Roof-Wall Connection II

The second roof-wall system proposed, which is particularly indicated for low quality dry stone masonry (where the stones used are small and the joints large), is the use of timber members to interconnect the different walls through the roofing system *while* holding the walls in place (Figure 6-9).

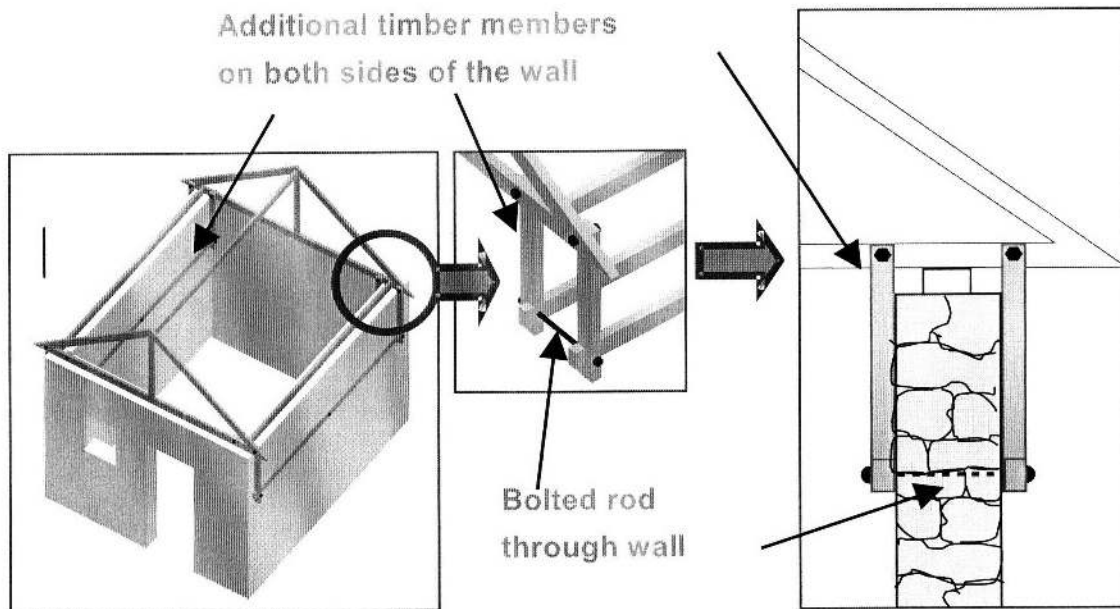


Figure 6-9. Roof-wall connection system using timber members (Drawings by: Yanni Loukissas).

6.3 Discussion

The first part of this chapter discussed a number of low-cost construction improvements that can be used in new unreinforced stone masonry structures. The introduction of through-stones and the use of large rectangular stones is the most efficient way to prevent two commonly occurring failure mechanisms, wall delamination and crumbling. Also, the importance of the proper dimensioning and distribution of wall openings has been described and a table with the proper opening dimensions provided. In addition, it has been explained that it is important to keep the centers of mass and stiffness of the structure close to each other to prevent the generation of torsional forces. This can be achieved by evenly distributing the openings around the structures. In addition, a series of retrofit systems have been described that can be used to strengthen existing structures. Finally, a possible low-cost implementation of “Hanchiku,” an ancient Chinese base isolation system, has been suggested as a foundation system with isolation properties. A simpler but as yet untested high frequency filter obtained by introducing rubber pieces at the foundation level, has been proposed to provide a simple, low-cost limited base isolation.

A number of simple retrofit systems for unreinforced stone masonry have been suggested in the second part of this chapter. As for new construction, the insertion in the walls of through-stones is an efficient and cost-effective way to strengthen two-wythe walls. Furthermore, to reduce the risk of out-of-plane failure of long unsupported walls, the construction of partition walls has been recommended. Finally, two wall-roof connection arrangements have been provided for bonding together the individual walls and achieving an overall box behavior of the structure.

Chapter 7

7. Conclusions and Future Work

This preliminary research has shown that, in spite of having a small energy content and being far from the natural frequencies of structures, the high frequency components of earthquake vibrations can be the source of significant structural damage to unreinforced masonry. Moreover, our tests have proven that the higher frequency waves travelling through stiff masonry structures can trigger two types of failure mechanisms that have not yet been taken into account.

The first failure mechanism is associated with the fact that high frequencies can cause small vertical inter-stone vibrations that result in irreversible relative displacements (ratcheting) of the stones, causing the wall to deform and ultimately collapse. The energy needed to cause this deformation and failure of the walls originates from gravitational forces contained in the structure itself, this potential energy is released by the high frequency inter-stone vibrations. The stone wall tests have shown that significant wall deformations and partial failure occur at frequencies and accelerations as low as 11Hz and 0.17g respectively. Experimental evidence indicates that at higher frequencies, the failure occurs significantly faster. In addition, the combination of both the vertical and the horizontal accelerations was the most detrimental. The reduction of frictional forces between the masonry resulting from the vertical accelerations compounded the deformational effect of the horizontal thrust resulting from the horizontal acceleration.

Second, the significant increase of outward thrust generated by the shear fluidization and densification process of the granular material making up the inner core of a wall can contribute to the structural failure. A series of dynamic tests on two-wythe brick walls with granular infill have shown the following trends. When the walls were vibrated vertically, the failure onset by overturning occurred at heights 20%-30% lower than in the static case. A failure height reduction of 30%-40% was observed when the walls were vibrated horizontally. Two-wythe stone walls, found in domestic architecture and monumental structures, will be the most affected by this failure mechanism. Also, analytical tests have shown introducing through-stones in the wall can significantly mitigate wall delamination, one of the dominant failure mechanisms of dry stone

masonry. Moreover, the larger the number of through-stones introduced, the more the stability *and* the ductility is enhanced.

These two new failure mechanisms will need to be integrated with other known masonry failure mechanisms to improve the performance of low-cost housing and retrofit schemes. A number of simple, low-cost remedial actions have been illustrated that can be used to reduce the risk of wall delamination, crumbling, and out-of-plane failure: insertion of through-stones, use of larger stone units (especially at the corners) and cementitious mortars, rendering of stone units, and the proper connection of the roof with the walls. It is important to note that the combination these construction improvements will make the structure more stable in case of a seismic event, but it will not make it earthquake-proof. To further improve the dynamic performance of the structure it would need to be reinforced with a RC or steel frame.

After establishing that higher frequencies / low energy seismic vibrations can have a detrimental effect on unreinforced mortar-less stone or brick masonry, it is important to conduct additional tests to better understand and quantify these two new failure mechanisms. Future work should investigate:

- Damage progression with respect to time at a given fixed vibration frequency
- Top-constrained walls
- Significance of the masonry unit size and shape
- Performance of bands in the walls
- Addition of core infill cohesion

Bibliography

- Arya, S., 2005. "Earthquake Resistant Reconstruction and New Construction of Masonry Buildings in Jammu & Kashmir State. Ministry of Home Affairs, Government of India. <http://ndmindia.nic.in/EQProjects/Kashmir%20Final.pdf>
- Azevedo, J. and Sincaian, G., 2005. "Modeling the Seismic Behavior of Monumental Masonry Structures." Instituto Superior Tecnico, Lisboa, Portugal.
- Braile, Larry, 2005. "Explorations in Earth Science." Purdue University. Downloaded from: <http://web.ics.purdue.edu/~braile/educindex/educindex.htm>.
- Carson, J.W. and Jenkyn, R.T., 2005. "Load Development and Structural Considerations in Silo design." Jenike & Johanson Inc., Westford, MA. Downloaded from www.jenike.com.
- CHRR, 2005. Center for Hazards & Risk Research, Columbia University. Downloaded from: <http://www.ldeo.columbia.edu/chrr/research/hotspots/maps.html>.
- CIRES, 2001. "January 2001 Bhuj Earthquake, Gujarat, India." Downloaded from: <http://cires.colorado.edu/~bilham/Gujarat2001.html>.
- CUL, 2005. "Guide for Earthquake Resistant Detailing." City University, London. Downloaded from: <http://www.staff.city.ac.uk/earthquakes/Earthquakes/Earthquakes.htm>
- D'Ayala, Dina and Kansal, Ashima, 2004. "Analysis of seismic vulnerability of the architectural heritage of Bhuj."
- Felice, G., 2004. "Out-of-plane fragility of historic masonry walls".
- Fukuyama, E., Madariaga, R., 1999. "Dynamic Rupture Front Interaction on 3D Planar Fault." National Institute for Earth Sciences and Disaster Prevention, Tsukuta, Japan.
- Giordano, A Elena Mele, and Antonello De Luca, 2005. "Numerical Modelling of Masonry Structures Through Deifferent Approaches." Universita degli Studi di Napoli, Italy.
- Gomes, E. and Hossain, I., 2003. "Transition from Traditional Brick Manufacturing to More Sustainable Practices." Energy for Sustainable Development, Volume VII, No. 2.
- Government Code (2004). Bill number: AB 2533, An act to amend Section 8875.8 of the Government Code, relating to seismic safety, February 20, 2004.
- Gudehus, G. (2004). "Seismic decay of psammoids and pleoids with and without hypoplasticity." Institute of Soil Mechanics and Rock Mechanics, University of Karlsruhe, Germany.

- Gupta, Harsh K., Bhattacharya, S.N., Kumar, R.M., and Sarkar, D., 1998. "Pokhran and 28 May 1998 Chaghai Nuclear Explosions." National Geophysical Research Institute, Hyderabad, India. Downloaded from: <http://www.iisc.ernet.in/currsci/apr25/articles20.htm>
- Huntley, J.M. (1998). "Fluidization, Segregation and Stress Propagation in Granular Materials." The Royal Society. 356, 2569-2590 (2569).
- Kambod A. Hosseini et al., 2004. "Engineering Geology and Geotechnical Aspects of Bam Earthquake." International Institute of Earthquake Engineering and Seismology, Iran.
- Keppler, Istvan. "Finite Element Simulation of Arching in Granular Assemblies." Szent Istvan University, Faculty of Mechanics and Engineering Design, Hungary.
- Kolb, E., Mazozi, T., Clement, E., Duran, J., 1999. "Force Fluctuations in a Vertically Pushed Granular Column." Universite Pierre et Marie Curie, Paris, France.
- Kumar, Jyant, 2001. "Seismic passive earth pressure coefficients for sands". Canadian Geotechnical Journal. 38(4): 876-881.
- Massarsch, K. R., 2005. Geoforum, 2005. Available from: <http://www.geoforum.com/knowledge/texts/compaction/viewpage.asp?ID=29>
- Marroquin, F.A. and Herrmann, H.J., 2003. "Ratcheting of Granular Material." Physical Review Letters, Volume 92-5, 05301-1.
- Murthy, C.V.R., 2003. IITK-BMTPC Earthquake Tips Series. Downloaded from: http://www.nicee.org/EQTips/IITK_BMTPC.htm
- Ni, Zhiping, 1997. "An Expert System for Analysis of Grain Bin Loads." The University of Manitoba, Canada.
- Niedostatkiewicz, Maciej, 2005. Department of Geotechnical Engineering, University of Karlsruhe, Karlsruhe, Germany.
- OSHA, 2004. Wyoming Workers' Safety. Downloaded from: <http://159.238.91.226/oshapamphlets/guidebooklet.pdf>
- Penna, A., 2004. "Seismic assessment of masonry structures by non-linear macro-element analysis."
- Plate Tectonic, 2005. "Earth's Moving Force." Downloaded from: http://www.msnucleus.org/membership/html/k-6/pt/earthquakes/3/pte3_1a.html
- Schulze, D, 2005. "Stresses in Silos." Downloaded from: <http://www.dietmar-schulze.de/spanne.html>

- Singh, J.P., 2005. "Vertical Motions and Design Time Histories" JP Singh and Associates, California, <http://nisee.berkeley.edu/lessons/nearsources.html>.
- Soil Compaction Handbook. Downloaded on September 7, 2005 from: http://www.concrete-catalog.com/soil_compaction.html
- Richards, R., Elms, D. G. and Budhu, M., 1990. "Dynamic fluidization of Soils", Journal of Geotechnical Engineering, ASCE, Vol. 116(5), pp.740-759.
- Stewart, J.P., Chiou, S.J., Bray, J.D., Somerville, R.W., Abrahamson, N.A., 2001. "Ground Motion Evaluation Procedures for Performance-Based Design." PEER Report 2001/09, University of California, Berkeley.
- Svinkin, Martin R. 1999. "24th Annual Member's Conference of the Deep Foundations Institute in Dearborn, Michigan.
- Take, W.A. and Valsangkar, A.J., 2001. "Earth Pressures on Unyielding Retaining Walls of Narrow Backfill Width." Canadian Geotechnical Journal: 38(6): 1220-1230.
- UN-Habitat, 2005. Human Settlements Statistic. Retrieved on 10/31/2005 from: <http://hq.unhabitat.org/register/shop.asp>.
- UNCHS, 1999. Basic Facts on Urbanization, Nairobi, table 9.
Downloaded from: <http://www.habitat.org/how/intlstats.aspx>.
- US Army Corps of Engineers, 1994. "Stability of Gravity Walls: Vertical Shear. Department of the Army Washington, DC, Technical Letter No. 1110-2-352.
- US Army Corps of Engineers, 2005. Publication: EM 1110-2-2502. Retrieved on 09/20/2005 from <http://www.usace.army.mil/usace-docs/eng-manuals/em1110-2-2502/toc.htm>
- Velez, L.F.R., 2003. "A Simplified Mechanics-Based Procedure for the Seismic Risk Assessment of Unreinforced Masonry Buildings." European School of Advanced Studies in Reduction of Seismic Risk, Pavia, Italy.
- Xyoli Perez-Campos, 2002. "A Comprehensive Study of the Radiated Seismic Energy". Stanford University.

Appendix 1: UDEC Scripts

```
;GENERATE BLOCK
  ro 0.002
  block 0,0 0,1.27 1.02,1.27 1.02,0
;DEFINE MATERIAL PROPERTIES 1
  prop mat=1 dens=2000
  prop jmat=1 jkn=1.33e12 jks=1.33e12 jfric=55.0
;SUBDIVIDE BLOCK
  cr 0,0.05 1.02,0.05
  cr 0.4,0.05 0.4,1.27
  cr 0.5,0.05 0.5,1.27
  cr 0.52,0.05 0.52,1.27
  cr 0.62,0.05 0.62,1.27
  fix range 0,1.02 0,0.05
;DELETE UNWANTED BLOCKS
  de ran 0,0.4 0.05,1.27
  de ran 0.62,1.02 0.05,1.27
;DEFINE MATERIAL PROPERTIES 2
  change mat 2 range x 0.41,0.49 y 0.051,1.27
  prop mat=2 dens=2000
  prop jmat=2 jkn=1.33e12 jks=1.33e12 jfric=55.0
  change mat 3 range x 0.53,0.61 y 0.051,1.27
  prop mat=3 dens=2000
  prop jmat=3 jkn=1.33e12 jks=1.33e12 jfric=55.0
;GENERATE THE GRANULAR INFILL
  vo edge 0.12 iter 100 range mat 3
  vo edge 0.12 iter 100 range mat 2
  set gravity 0 -9.81
;RECORD A MOVIE
  title 'Stone STATIC SS X&Y F100000 A0.0005/Friction 55'
  ;movie on fi movies\Stone F10000000 Amp0005.dcx st 100000
```



```

;PLOT VELOCITY
    ;plot hold block vel
    damp 0.0001 0.1
;DEFINE SINOSOIDAL LOADING IN X AND Y
    def _find_block
        _iab = b_near(0.42, 0.0)
    end
    _find_block
    def _mark_time
        starttime = time
    end
    _mark_time
    def pulse1
        whilestepping
            dytime = time - starttime
            xwave = 2.0*pi*freq*ampl*cos(2.0*pi*freq*dytime)
            ywave = 2.0*pi*freq*ampl*cos(2.0*pi*freq*dytime)
            b_yvel(_iab) = ywave
            b_xvel(_iab) = xwave
        end
;ENTER LOADING PARAMETERS
    set freq=10 ampl=0.0005
;CREATE A TITLE AND A MOVIE
    title 'Stone STATIC SS X&Y F100000 A0.0005/Friction 55'
    movie on fi movies\Stone F10000000 Amp0005.dcx st 100000

```

Appendix 2: Pamphlet Distributed in Kashmir 06

This simple pamphlet was developed partially guided by the findings of this research to address the needs of those who would have to rebuild their houses without any external support of any kind.

بِسْمِ اللّٰهِ الرَّحْمٰنِ الرَّحِیْمِ

زیادہ مضبوط پتھر کے گھر بنانے کے بنیادی قاعدے

جیسے جنبش میں بو بہ ارزو سامان قصر سلطان گرا نہیں سکتا ہم نے بنیاد رکھی جس گھر کی کوئی طوفان بلا نہیں سکتا

دوبارہ نہ ہونے دیجیے!



مزید معلومات کے لیے: www.engineering4theworld.org/Pakistan.html

مسئلہ: دیوار کا گرنا
حل: دیواروں کو چھت کے ساتھ مضبوطی سے جوڑنا

آسان طریقہ: لوہے یا عمارتی لکڑی کے لمبے ٹکڑے دیواروں میں ڈال کر انہیں تار کے ساتھ چھت کے ڈھانچے سے جوڑ دیں



زیادہ مضبوط طریقہ: عمارتی لکڑیوں کے سریوں سے ایک ڈھانچا بنائیں جو دیوار کو دونوں طرف سے پکڑے اور چھت سے بھی جڑا ہوا ہو



دیوار کے دونوں طرف لگے لکڑی کے سریوں کو جوڑنے کے لیے دیوار کے اندر بیچ یا بولٹ ڈالیں

مسئلہ: دیوار کے ٹکڑے ٹکڑے ہو جانا
حل: بڑے پتھر جن کی لمبائی دیوار کی چوڑائی کے برابر ہو

صحیح! غلط!



مسئلہ: کمزور دیواریں
حل: دیواروں اور کھڑکیوں کے ناپ کا ٹھیک تناسب



کہار مثال کے طور پر دکھایا گیا ہے۔ اب طول و عرض بدل سکتے ہیں لیکن ضروری ہے کہ تناسب یہ ہی رہے

چوکور پتھر



پوری دیوار میں پتھروں کے بیچ کم سے کم جگہ ہونی چاہیے

یہ گھر مثال کے طور پر دکھایا گیا ہے۔ اب طول و عرض بدل سکتے ہیں لیکن ضروری ہے کہ تناسب یہ ہی رہے

گول ہموار
سطح کے پتھر مت استعمال کریں

بڑے چوکور پتھروں کا استعمال کریں

بڑے چوکور پتھروں کا استعمال کریں

